Table 2. Virus Titers in Mice Infected With Wild-Type and Neuraminidase 117 Mutant Viruses

Time After Infection	Virus	Treatment[a]	Virus Titer (log_{10} PFU/g)					
			Brain	Liver	Spleen	Kidney	Jejunum	Nose
Day 3	VN1203 wtNA-117I	Mock	...[b]	...	4.5 ± 0.7	2.3	...	...
		Oseltamivir	...	...	...	...	...	...
	VN1203 NA-117V	Mock	...	...	3.7 ± 0.2	2.0	...	...
		Oseltamivir	...	...	...	...	...	...
	TY114 wtNA-117V	Mock	...	...	...	...	...	...
		Oseltamivir	...	...	...	...	...	...
	TY114 NA-117I	Mock	...	...	...	...	...	...
		Oseltamivir	...	...	...	...	...	...
Day 6	VN1203 wtNA-117I	Mock	6.1 ± 1.3	2.5 ± 0.7	3.1 ± 0.2	5.8 ± 0.3	...	4.7 ± 0.1
		Oseltamivir	...	...	...	...	...	...
	VN1203 NA-117V	Mock	7.4 ± 1.1	4.6 ± 0.9	4.3 ± 0.6	7.8 ± 0.7	3.3, 5.6	6.5 ± 2.0
		Oseltamivir	...	...	2.5	...	...	7.2
	TY114 wtNA-117V	Mock	...	...	2.6, 2.5	...	...	2.6, 2.8
		Oseltamivir	...	...	2.8	...	...	2.8
	TY114 NA-117I	Mock	2.9	...	3.3 ± 0.1	...	3.2	2.6 ± 0.2
		Oseltamivir	...	...	...	...	...	...

Data are mean ± SD (n = 3).

Abbreviation: PFU, plaque-forming units.

[a] Mice were intranasally infected with ten 50% mouse lethal doses of virus and then mock treated (with distilled water) or treated with oseltamivir carboxylate (300mg/kg) 2 h after infection and then twice daily for 5 d.

[b] Virus not detected (detection limit, <2.0 log_{10} PFU/g).

oseltamivir, we performed molecular dynamics simulations. First, we assessed the equilibration of the trajectories by monitoring the root-mean-square deviations of all backbone heavy atoms from the initial structure as a function of simulation time (Supplementary Figure 1). Both the wild-type and the NA-117V systems reached equilibrium within 2.5 ns. Therefore, the trajectories extracted from the 2.5 to 5.0 ns simulations were used in subsequent analyses. Second, we compared the binding free energy difference between the wild-type and I117V mutant, which was calculated using the MM/PBSA method [31] (Table 3). This method has previously provided useful information regarding the binding affinity of oseltamivir to various NAs of influenza viruses [25–28]. The estimated binding free energies ($\Delta G_{binding}$) were −19.73 and −16.05 kcal/mol for the wild-type and I117V mutant, respectively. These values indicate qualitatively good agreement with the experimental binding free energies ($\Delta G_{binding,exp}$), which were estimated from the IC_{50} values. Thus, our energy analysis shows that the I117V substitution causes a lower binding affinity of oseltamivir carboxylate for the I117V mutant.

To further investigate the effect of the I117V substitution on the interaction with oseltamivir, we analyzed the percentage occupation of hydrogen bonds between oseltamivir and NA during the simulation (Figure 3*B* and Supplementary Table 2). Hydrogen bonds were assigned by using the ptraj program in AMBER 11 on the basis of the following criteria [26]: the distance between the proton donor and acceptor atoms was ≤3.5 Å, and the angle formed by the donor, hydrogen, and acceptor was ≥120°. Unlike the wild-type simulation, no hydrogen bonds were observed between R118 and the carboxyl group of oseltamivir in the simulation of the I117V mutant (Figure 3*B*). The preferential distances of O_2-NH_1 (R118) and O_2-NH_2 (R118) in the wild-type were 3.80 and 2.85 Å, respectively, whereas those in the I117V mutant were 5.45 and 5.30 Å, respectively (Figure 3*C*). Of note, the preferential distances of N_2-OE_1 (E119) were not different between the wild-type and mutant viruses. Since valine is smaller than isoleucine by 1 methylene group, the substitution of isoleucine for valine at position 117 could induce a slight distortion around residue 117 because of the loss of van der Waals contacts. This local change in molecular structure may be responsible for the change in orientation of R118 relative to oseltamivir. As a result, the loss of the hydrogen bond because of the I117V substitution would lead to the reduced susceptibility to oseltamivir.

DISCUSSIONS

Here, we found that an Ile-to-Val change at position 117 of NA substantially reduced the in vivo susceptibility to

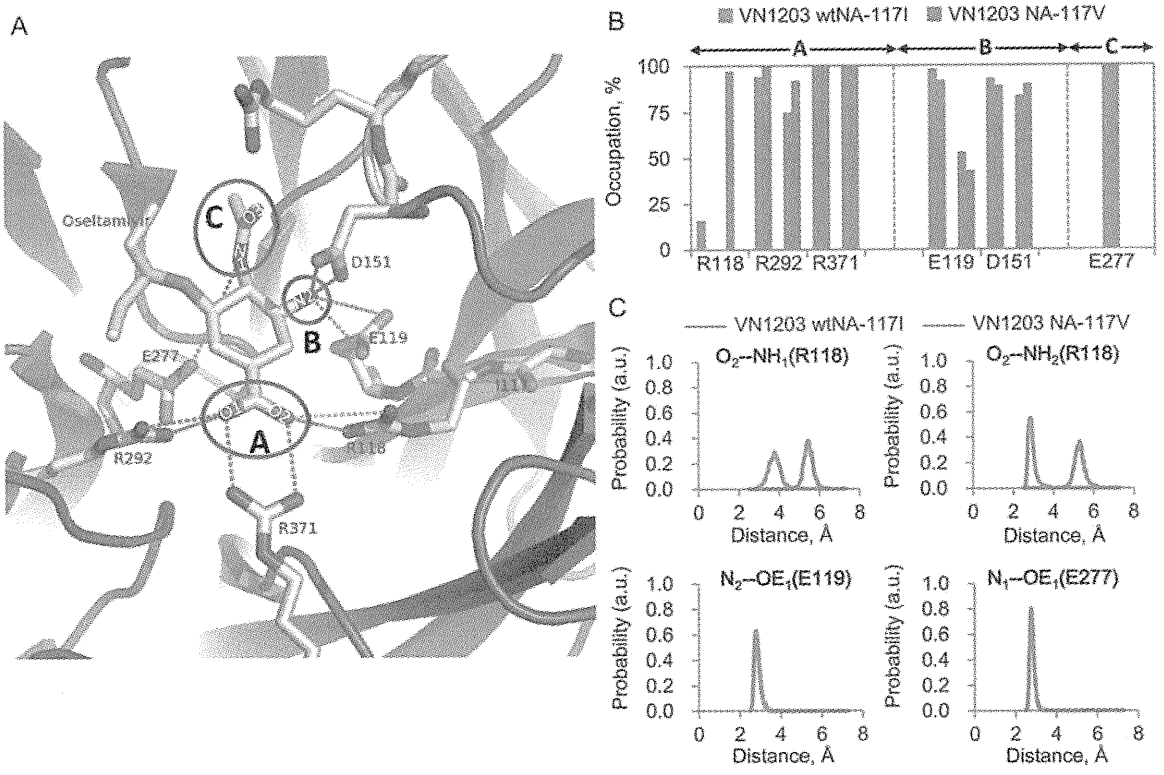

Figure 3. Hydrogen bonds between residues in the binding pocket of neuraminidase (NA) and oseltamivir predicted by using molecular dynamics simulation. *A*, Amino acid residues analyzed for hydrogen bonding are shown in the structure of the N1 NA in complex with oseltamivir. *B*, Percentage occupation pattern of hydrogen bonds between residues of oseltamivir and NA (defined in Figure 3*A*) for wild-type and I117V NA. *C*, Interatomic distances of hydrogen bonds between oseltamivir and residues R118, E119, and E277 of NA.

oseltamivir for 2 of 3 virus pairs tested, although, in vitro, the decrease in susceptibility to oseltamivir carboxylate induced by this mutation was only a few fold (1.3- to 6.3-fold). Compared with substitutions such as H274Y or D292N, which are selected under drug pressure and increase IC_{50} values by at least 100-fold, the I117V mutation does not dramatically affect the in vitro susceptibility to oseltamivir. However, this mutation did affect the survival of the oseltamivir-treated mice (Figure 2). This discrepancy between in vitro and in vivo susceptibility to oseltamivir was previously reported by Govorkova et al [32], who found that strains that differ by only 2-fold in the IC_{50} of oseltamivir carboxylate in vitro differ substantially in their oseltamivir susceptibility in mice, as evaluated by lethality; our data are consistent with these findings.

Table 3. Free Energy of Binding Between Oseltamivir and Neuraminidase by Using the Molecular Mechanics/Poisson-Boltzmann Surface Area Method

Contribution	VN1203 wtNA-117I	VN1203 NA-117V
ΔE_{elec}	−185.68	−171.78
ΔE_{vdw}	−30.37	−31.42
ΔG_{sol}	175.09	167.54
$\Delta G_{sol(ele)}$-E_{ele}	−2.83	−2.78
-$T\Delta S$(total)	24.06	22.39
$\Delta G_{binding}$	−19.73	−16.05
$\Delta G_{binding,exp}$[a]	−13.10	−11.90

[a] Calculated from the half maximal inhibitory concentration (IC_{50}) by using the following formula: $\Delta G_{binding,exp} = RT\ ln\ K_{dissociation} = RT\ ln(IC_{50} + 0.5\ C_{enzyme}) \sim RT\ ln\ IC_{50}$, where R is the ideal gas constant, T is the temperature in K, and *C enzyme* is the concentration of the enzyme, which is very small after equilibration is reached and can be omitted in most cases. IC_{50} values of 0.32 nM (VN1203 wtNA-117I) and 2.0 nM (VN1203 NA-117V) were used to calculate $\Delta G_{binding,exp}$.

The effects of the I117V substitution on susceptibility to oseltamivir also differed among the 3 virus backbones tested, both in vitro and in vivo. A previous study showed that clade 1 viruses are more sensitive to oseltamivir than are clade 2 viruses [9]. When we compared the VN1203 pair (clade 1), the NA-I117V mutation caused a 6.3-fold decrease in susceptibility to oseltamivir in vitro and a 60% decrease in the survival of mice treated with oseltamivir at the highest dose tested. On the other hand, for the TY114 and VN31412 pairs (both clade 2.3.4), modest increases in IC_{50} values induced by the I117V mutation were observed (1.3- and 3.4-fold decreases). In addition, although the increase in IC_{50} values caused by the

I117V mutation was smaller for the TY114 pair than for the VN31412 pair, decreases in the therapeutic effect of oseltamivir in mice were observed for TY114 but not for VN31412. There are 19 amino acid differences between the NA proteins of VN1203 and TY114. The NA of TY114 and that of VN31412 differ by 2 amino acids, at positions 16 and 42; however, these residues are located in the NA transmembrane and stalk domain, respectively, and are not thought to be involved in the binding between NA and oseltamivir [33, 34]. Given that the virulence of an H5N1 virus strain is one factor that determines the therapeutic efficacy of oseltamivir in mice [35], this strain difference in oseltamivir efficacy in mice may be due to differences in pathogenicity rather than to these amino acid differences, because VN31412 is more virulent than TY114 by 10-fold on the basis of MLD_{50} values. Our results indicate that the NA-I117V mutation does not alter susceptibility to oseltamivir dramatically but compromises the effectiveness of the drug in virus strains that are more sensitive to oseltamivir or are of low pathogenicity in mice.

Molecular dynamics simulation demonstrated that NA-I117V induces the loss of hydrogen bonding between NA R118 and the carboxyl group of oseltamivir, although this did not lead to a global conformational change in the binding between oseltamivir and NA. This slight conformational change did, however, result in a lower binding affinity of the enzymatic site of NA for oseltamivir, providing a structural basis for the reduced sensitivity to oseltamivir caused by this mutation. A review of the influenza sequence database revealed that a few viruses possessing the mutation at position 117 in NA were isolated in East Asian countries, like Bangladesh, Bhutan, and India, from 2010 to 2011 (Supplementary Table 1). Remarkably, most of these viruses were avian isolates, suggesting that this mutation occurred sporadically during the course of the evolution of the viruses that prevail among poultry and not as a result of oseltamivir treatment. Given the wide range of H5N1 clades/subclades in which genetic variation has been observed at residue 117 of NA, it would be important to assess the effects of introducing this mutation into a more diverse set of H5N1 virus NAs, particularly clade 2.2 and 2.1, which have been implicated in a large number of human infections with H5N1 viruses.

In summary, we examined the effect of the NA-I117V mutation on susceptibility to oseltamivir in vitro, in vivo, and in silico and determined that the I117V mutation is a genetic variation that reduces susceptibility to oseltamivir slightly in vitro but dramatically in vivo. This mutation results in the loss of a hydrogen bond between residue R118 and oseltamivir carboxylate, resulting in a lower binding affinity between oseltamivir carboxylate and NA. Importantly, the I117V mutation appears to arise not as a result of oseltamivir treatment but because of genetic drift among poultry—a finding that justifies the continued global surveillance of H5N1 viruses among poultry. Although an H5N1 virus with the I117V mutation was attenuated in a ferret model [12], given the spontaneous emergence of viruses with the I117V mutation and their potentially reduced sensitivity to oseltamivir, our findings are of value to those who treat patients infected with H5N1 viruses.

Supplementary Data

Supplementary materials are available at *The Journal of Infectious Diseases* online (http://jid.oxfordjournals.org/). Supplementary materials consist of data provided by the author that are published to benefit the reader. The posted materials are not copyedited. The contents of all supplementary data are the sole responsibility of the authors. Questions or messages regarding errors should be addressed to the author.

Notes

Acknowledgments. We thank Susan Watson for editing the manuscript.

Financial support. This work was supported by a grant-in-aid for Specially Promoted Research and by a contract research fund for the Program for Funding Research Centers for Emerging and Reemerging Infectious Diseases from the Ministries of Education, Culture, Sports, Science, and Technology and by grants-in-aid of Health, Labor, and Welfare of Japan, by ERATO (Japan Science and Technology Agency), and by National Institute of Allergy and Infectious Diseases Public Health Service Research grants. R. T. was supported by Research Fellowships from the Japan Society for the Promotion of Science for Young Scientists. M. I. was supported by a Grant-in-Aid for Young Scientists (B) from MEXT of Japan.

Potential conflicts of interest. All authors: No reported conflicts.

All authors have submitted the ICMJE Form for Disclosure of Potential Conflicts of Interest. Conflicts that the editors consider relevant to the content of the manuscript have been disclosed.

References

1. Li KS, Guan Y, Wang J, et al. Genesis of a highly pathogenic and potentially pandemic H5N1 influenza virus in eastern Asia. Nature **2004**; 430:209–13.
2. World Health Organization. Cumulative number of confirmed human cases of avian influenza A/(H5N1) reported to WHO. http://www.who.int/influenza/human_animal_interface/en/. Accessed 21 October 2012.
3. Ungchusak K, Auewarakul P, Dowell SF, et al. Probable person-to-person transmission of avian influenza A (H5N1). N Engl J Med **2005**; 352:333–40.
4. Colman PM, Hoyne PA, Lawrence MC. Sequence and structure alignment of paramyxovirus hemagglutinin-neuraminidase with influenza virus neuraminidase. J Virol **1993**; 67:2972–80.
5. Ives JA, Carr JA, Mendel DB, et al. The H274Y mutation in the influenza A/H1N1 neuraminidase active site following oseltamivir phosphate treatment leave virus severely compromised both in vitro and in vivo. Antiviral Res **2002**; 55:307–17.
6. Kiso M, Mitamura K, Sakai-Tagawa Y, et al. Resistant influenza A viruses in children treated with oseltamivir: descriptive study. Lancet **2004**; 364:759–65.
7. de Jong MD, Tran TT, Truong HK, et al. Oseltamivir resistance during treatment of influenza (H5N1) infection. N Engl J Med **2005**; 353:2667–72.
8. Rameix-Welti MA, Agou F, Buchy P, et al. Natural variation can significantly alter the sensitivity of influenza A (H5N1) viruses to oseltamivir. Antimicrob Agents Chemother **2006**; 50:3809–15.

9. McKimm-Breschkin JL, Selleck PW, Usman TB, Johnson MA. Reduced sensitivity of influenza A (H5N1) to oseltamivir. Emerg Infect Dis **2007**; 13:1354–7.
10. Monto AS, McKimm-Breschkin JL, Macken C, et al. Detection of influenza viruses resistant to neuraminidase inhibitors in global surveillance during the first 3 years of their use. Antimicrob Agents Chemother **2006**; 50:2395–402.
11. Hurt AC, Selleck P, Komadina N, Shaw R, Brown L, Barr IG. Susceptibility to highly pathogenic A (H5N1) avian influenza viruses to the neuraminidase inhibitors and adamantanes. Antiviral Res **2007**; 73:228–31.
12. Ilyushina NA, Seiler JP, Rehg JE, Webster RG, Govorkova EA. Effect of neuraminidase inhibitor-resistant mutations on pathogenicity of clade 2.2 A/Turkey/15/06 (H5N1) influenza virus in ferrets. PLoS Pathog **2010**; 6:e1000933.
13. Yi H, Lee JY, Hong EH, et al. Oseltamivir-resistant pandemic (H1N1) 2009 virus, South Korea. Emerg Infect Dis **2010**; 16:1938–42.
14. Hurt AC, Leang SK, Speers DJ, Barr IG, Maurer-Stroh S. Mutations I117V and I117M and oseltamivir sensitivity of pandemic (H1N1) 2009 viruses. Emerg Infect Dis **2012**; 18:109–12.
15. Case DA, Darden TA, Cheatham TE III, et al. AMBER 11. San Francisco: University of California, **2010**.
16. Dolinsky TJ, Czodrowski P, Li H, et al. PDB2PQR: expanding and upgrading automated preparation of biomolecular structures for molecular simulations. Nucleic Acids Res **2007**; 35:W522–5.
17. Frisch MJ, Trucks GW, Schlegel HB, et al.. Gaussian 03, revision E.01. Wallingford, CT: Gaussian, **2004**.
18. Bayly CI, Cieplak P, Cornell WD, Kollman PA. A well-behaved electrostatic potential based method using charge restraints for determining atom-centered charges: the RESP model. J Phys Chem **1993**; 97:10269–80.
19. Wang J, Wang W, Kollman PA, Case DA. Automatic atom type and bond type perception in molecular mechanical calculations. J Mol Graph Model **2006**; 25:247–60.
20. Hornak V, Abel R, Okur A, Strockbine B, Roitberg A, Simmerling C. Comparison of multiple Amber force fields and development of improved protein backbone parameters. Proteins **2006**; 65:712–25.
21. Wang J, Wolf RM, Caldwell JW, Kollman PA, Case DA. Development and testing of a general amber force field. J Comput Chem **2004**; 25:1157–74.
22. Berendsen HJC, Postma JPM, Funsteren WF. Molecular dynamics with coupling to an external bath. J Chem Phys **1984**; 81:3684–90.
23. Ryckaert JP, Ciccotti G, Berendsen HJC. Numerical integration of the Cartesian equations of motion of a system with constraints: Molecular dynamics of n-Alkanes. J Comput Phys **1977**; 23:327–41.
24. Darden T, York D, Pedersen L. Particle mesh Ewald: An N·log(N) method for Ewald sums in large systems. J Chem Phys **1993**; 98:10089–92.
25. Masukawa KM, Kollman PA, Kuntz ID. Investigation of neuraminidase-substrate recognition using molecular dynamics and free energy calculations. J Med Chem **2003**; 46:5628–37.
26. Aruksakunwong O, Malaisree M, Decha P, et al. On the lower susceptibility of oseltamivir to influenza neuraminidase subtype N1 than those in N2 and N9. Biophys J **2007**; 92:798–807.
27. Malaisree M, Rungrotmongkol T, Nunthaboot N, et al. Source of oseltamivir resistance in avian influenza H5N1 virus with the H274Y mutation. Amino Acids **2009**; 37:725–32.
28. Wang NX, Zheng JJ. Computational studies of H5N1 influenza virus resistance to oseltamivir. Protein Sci **2009**; 18:707–15.
29. Le QM, Ito M, Muramoto Y, et al. Pathogenicity of highly pathogenic avian H5N1 influenza A viruses isolated from humans from 2003 to 2008 in Northern Vietnam. J Gen Virol **2010**; 91:2485–90.
30. Uhlendorff J, Matrosovich T, Klenk HD, Matrosovich M. Functional significance of the hemadsorption activity of influenza virus neuraminidase and its alteration in pandemic viruses. Arch Virol **2009**; 154:945–57.
31. Srinivasan J, Cheatham TE III, Cieplak P, Kollman PA, Case DA. Continuum solvent studies of the stability of DNA, RNA, and phosphoramidate-DNA helices. J Am Chem Soc **1998**; 120:9401–9.
32. Govorkova EA, Ilyushina NA, McClaren JL, Naipospos TS, Douangngeun B, Webster RG. Susceptibility of highly pathogenic H5N1 influenza viruses to the neuraminidase inhibitor oseltamivir differs in vitro and in a mouse model. Antimicrob Agents Chemother **2009**; 53:3088–96.
33. Luo G, Chung J, Palese P. Alterations of the stalk of the influenza virus neuraminidase: deletions and insertions. Virus Res **1993**; 29:141–53.
34. Mitnaul LJ, Castrucci MR, Murti KG, Kawaoka Y. The cytoplasmic tail of influenza A virus neuraminidase (NA) affects NA incorporation into virions, virion morphology, and virulence in mice but is not essential for virus replication. J Virol **1996**; 70:873–9.
35. Yen HL, Monto AS, Webster RG, Govorkova EA. Virulence may determine the necessary duration and dosage of oseltamivir treatment for highly pathogenic A/Vietnam/1203/04 influenza virus in mice. J Infect Dis **2005**; 192:665–72.

Journal of Virology

Virulence Determinants of Pandemic A(H1N1)2009 Influenza Virus in a Mouse Model

Ryuta Uraki, Maki Kiso, Kyoko Shinya, Hideo Goto, Ryo Takano, Kiyoko Iwatsuki-Horimoto, Kazuo Takahashi, Rod S. Daniels, Olav Hungnes, Tokiko Watanabe and Yoshihiro Kawaoka

J. Virol. **2013, 87(4):2226. DOI: 10.1128/JVI.01565-12.**
Published Ahead of Print 5 December 2012.

JVI
Journals.ASM.org

Virulence Determinants of Pandemic A(H1N1)2009 Influenza Virus in a Mouse Model

Ryuta Uraki,[a] Maki Kiso,[a] Kyoko Shinya,[b] Hideo Goto,[a] Ryo Takano,[a] Kiyoko Iwatsuki-Horimoto,[a] Kazuo Takahashi,[c] Rod S. Daniels,[d] Olav Hungnes,[e] Tokiko Watanabe,[f,g] Yoshihiro Kawaoka[a,f,g,h]

Division of Virology, Department of Microbiology and Immunology, Institute of Medical Science, University of Tokyo, Tokyo, Japan[a]; Department of Microbiology and Infectious Diseases, Kobe University, Hyogo, Japan[b]; Department of Infectious Diseases, Osaka Prefectural Institute of Public Health, Osaka, Japan[c]; Virology Division, MRC-National Institute for Medical Research, London, United Kingdom[d]; Department of Virology, Norwegian Institute of Public Health, Oslo, Norway[e]; ERATO Infection-Induced Host Responses Project (JST), Saitama, Japan[f]; Department of Pathobiological Sciences, University of Wisconsin—Madison, Madison, Wisconsin, USA[g]; Department of Special Pathogens, International Research Center for Infectious Diseases, Institute of Medical Science, University of Tokyo, Minato-ku, Tokyo, Japan[h]

A novel swine-origin H1N1 influenza virus [A(H1N1)pdm09 virus] caused the 2009 influenza pandemic. Most patients exhibited mild symptoms similar to seasonal influenza, but some experienced severe clinical signs and, in the worst cases, died. Such differences in symptoms are generally associated with preexisting medical conditions, but recent reports indicate the possible involvement of viral factors in clinical severity. To better understand the mechanism of pathogenicity of the A(H1N1)pdm09 virus, here, we compared five viruses that are genetically similar but were isolated from patients with either severe or mild symptoms. In a mouse model, A/Norway/3487/2009 (Norway3487) virus exhibited greater pathogenicity than did A/Osaka/164/2009 (Osaka164) virus. By exploiting reassortant viruses between these two viruses, we found that viruses possessing the hemagglutinin (HA) gene of Norway3487 in the genetic background of Osaka164 were more pathogenic in mice than other reassortant viruses, indicating a role for HA in the high virulence of Norway3487 virus. Intriguingly, a virus possessing HA, NA, and NS derived from Norway3487 exhibited greater pathogenicity in mice in concert with PB2 and PB1 derived from Osaka164 than did the parental Norway3487 virus. These findings demonstrate that reassortment between A(H1N1)pdm09 viruses can lead to increased pathogenicity and highlight the need for continued surveillance of A(H1N1)pdm09 viruses.

The swine-origin H1N1 influenza A virus [A(H1N1)pdm09], which emerged in Mexico and the United States in the spring of 2009, spread throughout 200 countries and caused the first human pandemic of the 21st century (1–3). In most cases, patients exposed to A(H1N1)pdm09 experienced mild infections. However, A(H1N1)pdm09 did cause severe disease in high-risk groups, including pregnant women, young children, older adults, and those with chronic lung disease, obesity, or other comorbidities (4–9). Many severe cases were also reported sporadically in individuals who did not have any of these risk factors and were otherwise healthy (6). However, it is not known whether these variations in disease outcome originated from differences in the pathogenicity of the A(H1N1)pdm09 viruses.

The virulence and host range of influenza A virus are determined by both host and viral factors. Two amino acids at positions 627 and 701 in PB2 are important for the adaptation of avian influenza virus to mammalian hosts (10–12). In the case of A(H1N1)pdm09 virus, whose PB2 protein originated from an avian-like Eurasian swine virus, a basic amino acid at position 591 of PB2, which is a newly identified mammalian-adapting amino acid, has been shown to compensate for the lack of amino acid substitutions at positions 627 and 701 of PB2 (13, 14) Moreover, we and others recently found that an amino acid change of aspartic acid to glycine at position 222 (H1 numbering) in hemagglutinin (HA), which altered receptor-binding specificity (15–19, 34), confers high virulence to A(H1N1)pdm09 viruses (19–21). Here, we asked whether A(H1N1)pdm09 virus possesses other as yet unknown molecular determinants of pathogenicity. To answer this question, we compared the virulence levels of five A(H1N1)pdm09 viruses isolated from patients with severe or mild symptoms. We then generated a series of reassortant viruses between two A(H1N1)pdm09 viruses that differ in their pathogenicities in mice and attempted to determine the viral factors responsible for the high pathogenicity.

MATERIALS AND METHODS

Cells. Madin-Darby canine kidney (MDCK) cells were grown in minimal essential medium (MEM) with 5% newborn calf serum. Human embryonic kidney 293T cells were maintained in Dulbecco's modified Eagle's medium (DMEM) with 10% fetal calf serum. Cells were maintained at 37°C in 5% CO_2. MDCK cells were used for growth kinetics assays, and 293T cells were used for plasmid-based reverse genetics, as described below.

Viruses. In this study, we used the following five A(H1N1)pdm09 viruses: A/California/04/2009 (Cal04), A/Norway/3568/2009 (Norway3568), A/Norway/3487/2009 (Norway3487), A/Osaka/164/2009 (Osaka164), and A/Lviv/N6/2009 (LvivN6). These viruses were isolated from patients who had no underlying risk factors for severe influenza; unfortunately, detailed medical records, including vaccination history, treatment, and medical support after the onset of influenza in these patients, were unavailable. Cal04, Norway3568, and Osaka164 were isolated from patients who exhibited mild influenza symptoms and recovered, whereas Norway3487 and LvivN6 were isolated from patients who experienced severe symptoms and died. All of these viruses were generated by reverse genetics (22).

Received 20 June 2012 Accepted 30 November 2012
Published ahead of print 5 December 2012
Address correspondence to Tokiko Watanabe, twatanabe@svm.vetmed.wisc.edu, or Yoshihiro Kawaoka, kawaoka@ims.u-tokyo.ac.jp.

doi:10.1128/JVI.01565-12

Plasmid-based reverse genetics. All viruses used in the study were generated by plasmid-based reverse genetics, as described previously (22). Briefly, viral RNA was extracted from the supernatants of virus-infected MDCK cells by using a QIAamp viral RNA minikit (Qiagen, Hilden, Germany). Extracted RNA was reverse transcribed with Superscript III (Invitrogen, Carlsbad, CA) and the universal primers specific for influenza A virus genes to generate cDNA. The resulting products were PCR amplified by using KOD Fx DNA polymerase (Toyobo, Osaka, Japan) with specific primers for each virus gene and cloned into a plasmid under the control of the human RNA polymerase I (Pol I) promoter and the mouse RNA Pol I terminator (Pol I plasmids). Mutations in the PB2 genes of Norway3487 virus were generated by PCR amplification of the respective RNA polymerase I PB2 construct with primers possessing the desired mutations. Primer sequences are available upon request. All constructs were sequenced to ensure the absence of unwanted mutations.

Growth kinetics assays. Triplicate wells of confluent MDCK cells were infected with viruses at a multiplicity of infection (MOI) of 0.0001 with MEM containing 0.3% bovine serum albumin (BSA) and 1 μg/ml tosylsulfonyl phenylalanyl chloromethyl ketone (TPCK) trypsin and incubated at 37°C. Supernatants were harvested at a given number of hours postinfection (hpi). Virus titers were determined by plaque assays with MDCK cells.

Mouse experiments. Six-week-old female BALB/c mice weighing 15 to 20 g (Japan SLC, Inc., Shizuoka, Japan) were used in this study. Baseline body weights were measured prior to infection. Four mice per group were anesthetized with isoflurane and then intranasally inoculated with 10^4, 10^5, and 10^6 PFU (50 μl) of virus. Body weight and survival were monitored daily for 14 days postinfection (dpi). The percentage of body weight change was calculated by comparing the weight of each mouse at each time point to its initial weight on day 0. The percentage of maximum body weight loss was determined by comparing the most reduced body weight of each mouse to its initial body weight. To assess virus growth in respiratory organs, 12 mice per group were infected intranasally with 10^4 or 10^5 PFU of viruses; at 1, 3, 6, and 9 dpi, three mice were euthanized and their lungs and nasal turbinates were collected, homogenized with MEM containing 0.3% BSA, and titrated in MDCK cells by plaque assays.

Our research protocol for the use of mice followed the University of Tokyo's Regulations for Animal Care and Use, which were approved by the Animal Experiment Committee of the Institute of Medical Science, the University of Tokyo.

Histopathological analysis. Twelve mice per group were anesthetized with isoflurane and then intranasally inoculated with 10^5 PFU (50 μl) of virus. At 1, 3, 6, and 8 dpi, three mice were euthanized and their lungs were preserved in 10% phosphate-buffered formalin for pathological examination. The formalin-fixed lungs were processed for paraffin embedding. The paraffin-embedded tissues were cut into 5-μm-thick sections. One section was stained by using hematoxylin-and-eosin (H&E). Additional sections were processed for immunohistological staining with an anti-influenza virus rabbit polyclonal antibody (R309; prepared in our laboratory). Specific antigen-antibody reactions were visualized by means of 3,3′-diaminobenzidine tetrahydrochloride and the Dako EnVision system (Dako Co., Ltd., Tokyo, Japan).

Virus purification and Western blotting. MDCK cells were infected with the Osaka164, Norway3487, or Osaka(3P+NP) viruses at an MOI of 5. [In "Osaka(3P+NP)," "3P" represents a complex of the three polymerases PB2, PB1, and PA.] Culture supernatants were harvested at 3, 6, 9, and 12 hpi and clarified by low-speed centrifugation (3,000 rpm, 15 min, 4°C). The supernatants were collected and ultracentrifuged through a 25% sucrose cushion (45,000 rpm, 1.5 h, 4°C), by using an SW41 Ti rotor (Beckman Coulter), and were then subjected to Western blotting.

Cells and viruses were lysed with protein sample buffer and then heated for 10 min at 95°C and immediately chilled on ice prior to SDS-PAGE. SDS-PAGE was performed on Mini protean Any kD TGX gradient gels (Bio-Rad) for 30 min at 200 V. Proteins were transferred electrophoretically to a polyvinylidene difluoride (PVDF) membrane (Millipore) in transfer buffer (100 mM Tris, 190 mM glycine, 10% [vol/vol] methanol). The membrane was rocked with Blocking One (Nacalai Tesque) for 1 h and then was incubated with an anti-influenza virus rabbit antibody (R309) and a β-actin antibody (clone AC-74; Sigma-Aldrich) for 1 h at room temperature, followed by three washes with phosphate-buffered saline (PBS) supplemented with 0.005% (vol/vol) Tween 20 (PBS-T). Finally, the membrane was incubated with ECL enhanced chemiluminescence anti-mouse IgG horseradish peroxidase-linked whole antibody from sheep (GE Healthcare) for 1 h at room temperature and then washed three times with PBS-T. The membrane was incubated with Chemilumi One Super (Nacalai Tesque), and chemical luminescent signals were visualized by means of a Versa Doc imaging system (Bio-Rad).

Statistical analysis. Differences in virus titers of supernatants, lungs, and nasal turbinates were statistically analyzed using Student's *t* test. Differences in mean maximum body weight loss in mice were also statistically analyzed by using Student's *t* test.

RESULTS

Comparison of the replicative ability and pathogenicity of A(H1N1)pdm09 viruses. As noted above, the amino acids at positions 591 and 222 of PB2 and HA, respectively, have been identified as determinants for mammalian adaptation and pathogenicity of A(H1N1)pdm09 (14, 19–21), yet our previous study suggested contributions of other viral proteins to the pathogenicity of A(H1N1)pdm09 viruses in mammals (19). We therefore compared the biological properties of five A(H1N1)pdm09 viruses isolated from patients who had no underlying risk factors for severe influenza: A/Norway/3487/2009 (Norway3487) and A/Lviv/N6/2009 (LvivN6), which were isolated from fatal cases, and A/California/04/2009 (Cal04), A/Norway/3568/2009 (Norway3568), and A/Osaka/164/2009 (Osaka164), which were isolated from mild cases. All of these viruses were generated by reverse genetics (22).

To assess the growth properties of these five viruses *in vitro*, MDCK cells were infected with the viruses at a multiplicity of infection (MOI) of 0.0001. Norway3568, Norway3487, LvivN6, and Cal04 grew well, and their maximum titers (1.9×10^8, 3.9×10^8, and 4.2×10^8 PFU/ml at 36 hpi and 4.9×10^7 PFU/ml at 48 hpi, respectively) were significantly higher than that of Osaka164 (1.6×10^7 PFU/ml at 36 hpi) ($P < 0.01$) (Fig. 1). We also compared the replicative abilities of these viruses in the respiratory organs of mice. Mice were infected with 10^5 PFU of viruses and euthanized; their organs were collected at 3 and 6 dpi for virus titration. At 3 dpi, the virus titers in the lungs of mice infected with Norway3487 or Cal04 were significantly higher than those of mice infected with Osaka164 ($P < 0.05$), and at 6 dpi, the virus titers in the lungs of mice infected with Norway3487, LvivN6, or Cal04 were significantly higher than those of mice infected with Osaka164 ($P < 0.05$). Titers in the nasal turbinates of mice infected with LvivN6 were significantly lower than those of mice infected with other viruses at either 3 or 6 dpi ($P < 0.05$) (Fig. 2).

We next examined the pathogenicity of the viruses in mice. Four mice per group were intranasally infected with each virus at 10^4, 10^5, and 10^6 PFU, and morbidity and mortality were observed for 14 days. Although none of the viruses tested was lethal to mice, the degree of body weight change among the virus-infected mice varied, depending upon the infecting virus strain (Fig. 3). In mice infected with 10^6 PFU, two viruses, Norway3487 and LvivN6, caused significantly severe body weight loss (mean maximum body weight losses of 29.4% ± 4.0% and 27.8% ± 4.6%, respectively), compared with mice infected with Cal04, Norway3568, or

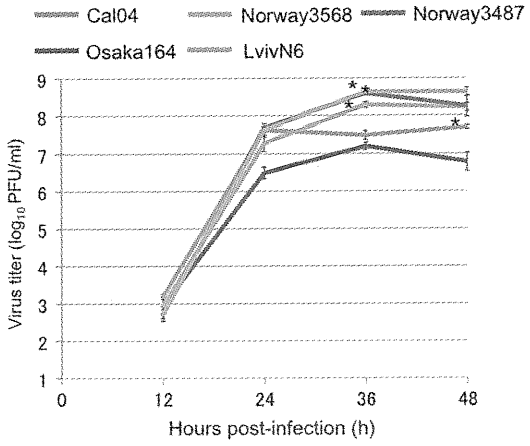

FIG 1 Growth kinetics of A(H1N1)pdm09 viruses in MDCK cells. MDCK cells were infected with five A(H1N1)pdm09 viruses at an MOI of 0.0001. At the indicated times after infection, virus titers in the supernatant were determined with MDCK cells. The reported values are means ± standard deviations (SD) from three independent experiments. Asterisks indicate that the maximum titers of Norway3568, Norway3487, LvivN6, and Cal04 were significantly higher than that of Osaka164 ($P < 0.01$).

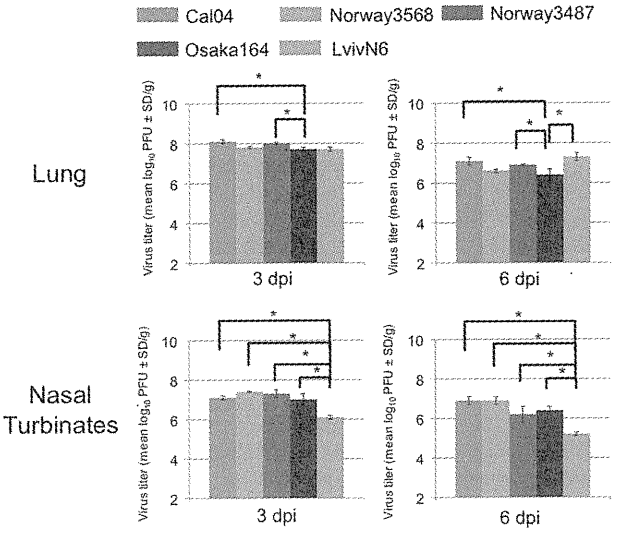

FIG 2 Virus titers in the respiratory tract of mice infected with A(H1N1)pdm09 viruses. Mice were intranasally inoculated with 10^5 PFU of each A(H1N1)pdm09 virus. Tissues were collected from mice ($n = 3$) on the indicated days postinfection (dpi), and titers were determined in MDCK cells. Asterisks signify significant differences in virus titers ($P < 0.05$).

Osaka164 (body weight losses of 16.0% ± 1.0%, 16.6% ± 3.3%, or 8.1% ± 3.9%, respectively) ($P < 0.05$) (Fig. 3A). In mice infected with 10^5 or 10^4 PFU of virus, Norway3487 still caused significantly severe body weight loss (28.9% ± 5.6% and 27.1% ± 4.8%, respectively) ($P < 0.05$), whereas mice infected with 10^4 PFU of LvivN6 experienced no substantial body weight loss (Fig. 3B and C) compared with viruses except for Norway3487. Taken together, our results revealed that Norway3487, which was isolated from a lethal human case, exhibited the highest pathogenicity in a mouse model, whereas Osaka164 (isolated from a mild case) showed the lowest pathogenicity in this animal among the viruses tested, suggesting the close correlation between clinical severity in humans and pathogenicity in mice. These results thus suggest that this mouse model is suitable for evaluating the pathogenicity of A(H1N1)pdm09 viruses.

The HA gene of Norway3487 virus contributes to high pathogenicity in mice. There are 10 amino acid differences between the genomes of Norway3487 and Osaka164 (Table 1). To determine which viral segment(s) contributes to virulence in mice, we generated a series of reassortant viruses between Norway3487 and Osaka164 (Table 2). These reassortant viruses were named according to the origin of their Osaka164 or Norway3487 genes. For example, "Norway(PB2)" indicates a virus possessing PB2 from Norway3487 and the rest of its genes from Osaka164. We first examined the *in vitro* replicative ability of the reassortants and their parental strains using MDCK cells. Three viruses possessing the HA of Norway3487 [i.e., Norway3487, Norway(HA), and Osaka(3P+NP)], had significantly higher replicative ability than Osaka164 ($P < 0.01$), whereas the replicative ability of the remaining reassortant viruses was similar to that of Osaka164 (Fig. 4). These results indicate that the HA of Norway3487 contributes to efficient replication in MDCK cells.

To examine the pathogenicity of the reassortant viruses in mice, we intranasally inoculated mice with 10^4 to 10^6 PFU of viruses and observed their mortality and morbidity for 14 days. The viruses possessing the HA of Norway3487 [i.e., Norway3487, Norway(HA), and Osaka(3P+NP)] caused more severe body weight loss than did Osaka164 (Table 2), whereas the other reassortant viruses caused body weight loss similar to that caused by Osaka164, suggesting that the HA gene has an important role in the increased pathogenicity of Norway3487 in mice.

The PB2 and PB1 genes of Osaka164 cause increased pathogenicity in mice in concert with the HA, NA, and NS genes of Norway3487. Intriguingly, as shown in Table 2, Osaka(3P+NP) was lethal to mice, with a 50% mouse lethal dose (MLD_{50}) of $10^{5.0}$ PFU, yet the parental pathogenic strain Norway3487 did not kill mice even when the mice were infected with the highest dose tested (i.e., 10^6 PFU/mouse). Since there are no amino acid differences in the PA, NP, M1, or M2 of Osaka164 and Norway3487, these results suggest that the expression of the PB2 and PB1 genes from Osaka164 and that of the HA, NA, and NS genes from Norway3487 enhance virulence in mice to a greater extent than the expression of these genes in the parental Norway3487 virus (Table 2). To better understand the difference in virulence in mice infected with Osaka164, Norway3487, and Osaka(3P+NP), we examined virus replication in the respiratory organs of mice. Mice were infected with 10^4 PFU of Osaka164, Norway3487, and Osaka(3P+NP), and virus titers were determined in the lungs and nasal turbinates at 1, 3, 6, and 9 dpi. For Osaka164, the virus titers in the lungs of the infected mice were lower than those of mice infected with other viruses, and no or low virus titers were recovered from the lungs or nasal turbinates, respectively, of the infected mice at 9 dpi (Table 3). On the other hand, although virulence differed between Osaka(3P+NP) and Norway3487, the virus growth properties in the lungs and nasal turbinates of infected mice were similar between these two viruses (Fig. 5 and Table 3).

We next analyzed the histopathology in the lungs of the virus-infected mice (Fig. 6). At 1 and 3 dpi, we did not observe any substantial histopathological differences in the lungs of the mice

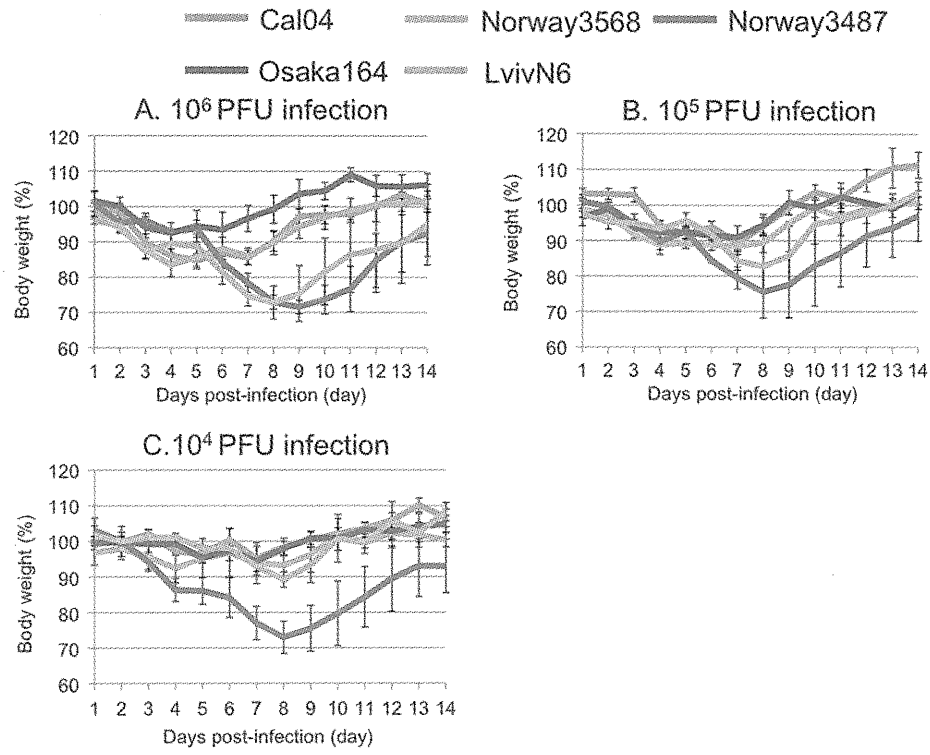

FIG 3 Body weight changes in infected mice. Four mice per group were intranasally inoculated with 10^6 (A), 10^5 (B), or 10^4 (C) PFU (each in 50 μl) of Cal04, Norway3568, Norway3487, Osaka164, or LvivN6. Body weights were monitored daily. The values represent average scores of overall body weight loss compared with initial body weight ± standard deviations (SD) from four mice.

infected with these viruses. However, differences between the Osaka(3P+NP) and other virus groups were observed at 6 dpi (Fig. 6); that is, the accumulation of neutrophils was more prominent in the Osaka(3P+NP)-infected mice (Fig. 6A and B) than in the other groups, whereas the lungs of mice infected with Norway3487 or Osaka164 virus exhibited lesions that included mononuclear cells, neutrophils, and regenerated epithelial cells (Fig. 6E and F, Norway3487, and I and J, Osaka164), indicating evidence of recovery from bronchopneumonia (Fig. 6). These data suggest that the Osaka(3P+NP) virus induced a longer active inflammatory process than did Norway3487 or Osaka164 virus. Of note,

TABLE 1 Amino acid differences between Osaka164 and Norway3487[a]

Protein	Position	Amino acid in:	
		Osaka164	Norway3487
PB2	340	K	N
	649	I	V
PB1	667	T	I
HA	125[b]	N	D
	203	S	T
	222	D	G
NA	248[c]	N	D
NS1	103	F	L
	123	I	V
NS2	63	K	E

[a] There were no amino acid differences in the PA, NP, PB1-F2, M1, and M2 proteins.
[b] H1 numbering.
[c] N1 numbering.

TABLE 2 Evaluation of virulence in mice infected with reassortants between Osaka164 and Norway3487[a]

Virus	MLD_{50}[b]	% of body wt loss (mean ± SD)[c]
Osaka164	$>10^{6.5}$	8.1 ± 3.9
Norway3487	$>10^{6.5}$	29.4 ± 4.0*
Norway(3P+NP)[d]	$>10^{6.5}$	9.1 ± 2.6
Osaka(3P+NP)	10^5	34.9*
Norway(PB2)	$>10^{6.5}$	13.2 ± 2.6
Norway(PB1)	$>10^{6.5}$	10.0 ± 2.8
Norway(PA)	$>10^{6.5}$	11.8 ± 1.1
Norway(NP)	$>10^{6.5}$	8.3 ± 3.1
Norway(HA)	$>10^{6.5}$	22.6 ± 3.4*
Norway(NA)	$>10^{6.5}$	9.7 ± 2.4
Norway(M)	$>10^{6.5}$	14.8 ± 4.1
Norway(NS)	$>10^{6.5}$	15.8 ± 4.3

[a] Mice were infected with 10^4, 10^5, or 10^6 PFU of reassortant viruses that combined the genes of the Norway3487 and Osaka164 viruses, generated by reverse genetics, with those of the parental Norway3487 and Osaka164 viruses.
[b] MLD_{50}, 50% mouse lethal dose.
[c] The mean maximum body weight losses ± standard deviations (SD) shown in the table are for mice that were infected with 10^5 PFU. Asterisks indicate that the mean maximum body weight loss was significantly severe in mice infected with the reassortant virus compared with that in mice infected with Osaka164 ($P < 0.05$).
[d] 3P, three-polymerase complex (i.e., PB2, PB1, and PA).

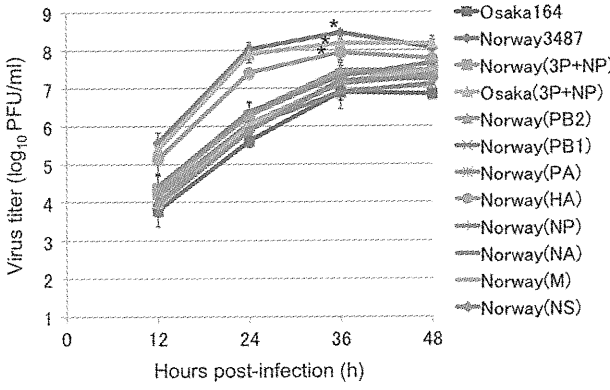

FIG 4 Growth kinetics of reassortant viruses in MDCK cells. MDCK cells were infected with reassortants between Osaka164 and Norway3487 at an MOI of 0.0001. At the indicated times after infection, virus titers in the supernatants were determined with MDCK cells. The reported values are means ± standard deviations (SD) from three independent experiments. Asterisks indicate that the maximum titers of Norway(HA), Osaka(3P+NP), and Norway3487 were significantly higher than that of Osaka164 ($P < 0.01$).

although there was no significant difference between the virus titers in the lungs of Norway3487 and Osaka(3P+NP) at 9 dpi (Table 3), viral antigen-positive cells in the lungs of mice infected with Osaka(3P+NP) were much more prevalent than those in the lungs of mice infected with Norway3487 at 8 dpi [Fig. 6C and D, Osaka(3P+NP), G and H, Norway3487, and K and L, Osaka164]. In addition, our *in vitro* study demonstrated that higher levels of M1 protein were expressed in MDCK cells infected with Osaka(3P+NP) than in those infected with Osaka164 or Norway3487 at 9 and 12 h postinfection ($P < 0.05$), yet there were no significant differences observed in viral protein levels in the culture supernatant of the cells infected with these viruses (Fig. 7). These results indicate that enhanced and/or sustained viral protein expression may contribute to pathogenicity in mice.

Amino acid substitutions in PB2 and PB1, in concert with HA, NA, and NS of Norway3487, contribute to high virulence in mice. There are only three amino acid differences between Osaka(3P+NP) and Norway3487: two in PB2 and one in PB1. To identify the molecular determinants responsible for the high virulence of Osaka(3P+NP) in mice, we tested three reassortant viruses, Osaka(PB2), Osaka(PB1), and Osaka(PB2/PB1), which possess PB2, PB1, or both genes from Osaka164, respectively, in the genetic background of Norway3487 (Fig. 5). We found that Osaka(PB2/PB1) was more pathogenic than Osaka(PB2) and Osaka(PB1): the MLD_{50} values for Osaka(PB2/PB1), Osaka(PB2), and Osaka(PB1) were $10^{4.3}$, $10^{5.5}$, and $10^{5.7}$ PFU, respectively (Fig. 5).

To further identify the amino acid that determines the high virulence of Osaka(3P+NP) in mice, we generated six mutant Norway3487 viruses possessing single or double point mutations at positions 340 and 649 of PB2 and position 667 of PB1 (Fig. 8) and examined their properties. We did not find any appreciable differences in the replicative abilities of all of these viruses in MDCK cells (data not shown) or in mice (Fig. 8 and Table 3). Furthermore, we did not find any significant difference in the polymerase activities in the minigenome assay (data not shown). Nonetheless, among the six viruses tested, Norway PB2 V649I/PB1 I667T and Norway PB2 N340K/PB1 I667T caused the highest mortality rates in mice, with MLD_{50} values of $10^{4.5}$ PFU and $10^{4.8}$ PFU, respectively (Fig. 8). The viruses with single point mutations in their PB2 or PB1 genes on the Norway3487 backbone were less pathogenic than Norway PB2 V649I/PB1 I667T or Norway PB2

TABLE 3 Virus titers in the respiratory tract of mice infected with reassortant viruses[a]

Virus	dpi	Virus titer (log_{10} PFU/g [mean ± SD]) in: Nasal turbinate	Lung
Osaka164	1	4.0 ± 0.6	6.9 ± 0.4
	3	6.0 ± 0.1	8.1 ± 0.5
	6	6.2 ± 0.2	7.1 ± 0.3
	9	4.2 ± 1.2	−[b]
Norway3487	1	5.4 ± 0.2	8.0 ± 0.2
	3	7.1 ± 0.3	8.5 ± 0.4
	6	6.3 ± 0.4	7.7 ± 0.2
	9	5.1 ± 1.1	4.8 ± 1.0
Osaka(3P+NP)	1	5.1 ± 0.4	7.9 ± 0.4
	3	6.3 ± 0.3	8.8 ± 0.3
	6	6.3 ± 0.6	7.6 ± 0.3
	9	5.4 ± 1.4	4.2 ± 0.7
Osaka(PB2)	1	4.7 ± 0.4	7.4 ± 0.2
	3	5.7 ± 0.7	8.3 ± 0.2
	6	5.3 ± 0.8	7.0 ± 0.2
	9	5.1 ± 1.7	4.0 ± 0.7
Osaka(PB1)	1	4.5 ± 0.4	7.3 ± 0.1
	3	7.2 ± 0.3	8.2 ± 0.3
	6	6.6 ± 0.3	7.3 ± 0.1
	9	5.3 ± 0.8	4.3 ± 0.4
Osaka(PB2/PB1)	1	4.8 ± 0.4	6.8 ± 0.4
	3	7.3 ± 0.4	8.4 ± 0.1
	6	6.7 ± 0.2	7.4 ± 0.1
	9	4.9 ± 0.2	4.7 ± 0.3
Norway PB2 N340K	1	4.4 ± 0.1	6.4 ± 0.1
	3	5.9 ± 0.8	8.2 ± 0.1
	6	6.2 ± 0.1	7.6 ± 0.3
	9	5.2 ± 0.5	4.6 ± 0.9
Norway PB2 V649I	1	5.1 ± 0.5	6.9 ± 0.1
	3	5.8 ± 1.5	8.1 ± 0.1
	6	5.6 ± 1.2	7.7 ± 0.1
	9	3.9 ± 0.8	6.0 ± 0.2
Norway PB2 N340K/V649I	1	4.1 ± 0.2	6.6 ± 0.4
	3	6.6 ± 0.6	8.5 ± 0.3
	6	5.6 ± 1.4	7.6 ± 0.1
	9	5.1 ± 1.8	5.1 ± 0.7
Norway PB2 N340K/PB1 I667T	1	5.0 ± 0.7	7.0 ± 0.1
	3	6.7 ± 1.1	8.3 ± 0.2
	6	6.6 ± 0.9	8.0 ± 0.2
	9	3.6 ± 0.7	4.9 ± 0.6
Norway PB2 V649I/PB1 I667T	1	4.2 ± 0.2	6.1 ± 0.3
	3	5.1 ± 0.8	7.9 ± 0.2
	6	5.5 ± 1.0	7.6 ± 0.3
	9	3.5 ± 0.7	3.8 ± 1.0
Norway PB2 N340K/V649I/PB1 I667T	1	4.5 ± 0.6	7.3 ± 0.3
	3	7.1 ± 0.3	8.1 ± 0.1
	6	6.1 ± 0.2	7.8 ± 0.1
	9	4.3 ± 0.7	4.3 ± 0.2

[a] Mice were intranasally inoculated with 10^4 PFU of Osaka164, Norway3487, or Osaka(3P+NP). Tissues were collected from mice ($n = 3$) on the indicated days postinfection (dpi), and titers were determined in MDCK cells.
[b] −, titer of <3.0 log_{10} PFU/g.

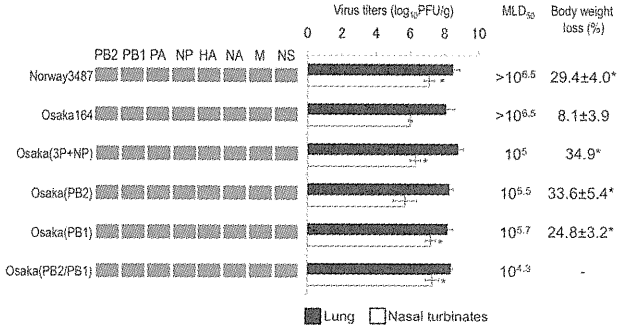

FIG 5 Characterization of reassortant viruses in mice. Mice were intranasally inoculated with 10^4 PFU of Osaka164, Norway3487, and reassortant viruses. Three mice per group were euthanized at 3 dpi, and virus titers in the lungs (■) and nasal turbinates (□) were determined by using plaque assays in MDCK cells. The results are expressed as mean titers ± standard deviations (SD). Asterisks indicate that virus titers in the nasal turbinates of mice infected with Norway3487 or reassortant viruses were significantly higher than those in the respiratory tract of mice infected with Osaka164 ($P < 0.05$). MLD_{50} values were calculated by observing mice infected with 10^4, 10^5, or 10^6 PFU of parental or reassortant viruses. The mean maximum body weight losses (%) ± standard deviations (SD) shown are for mice that were infected with 10^5 PFU. Asterisks indicate that the mean maximum body weight loss was significantly severe in mice infected with the reassortant virus, compared with that in mice infected with Osaka164 ($P < 0.05$). The minus sign indicates that the maximum body weight loss could not be measured because all of the infected mice died.

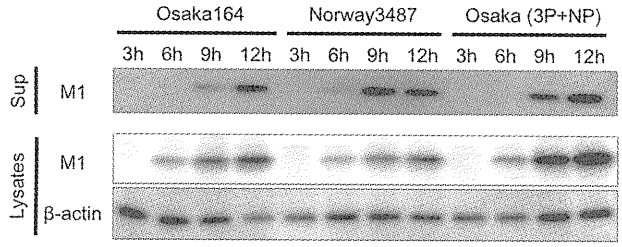

FIG 7 Viral protein expression levels in cell lysates and culture supernatants of cells infected with viruses. MDCK cells were infected with Osaka164, Norway3487, or Osaka(3P+NP) viruses at an MOI of 5, and samples were collected at 3, 6, 9, and 12 hpi. Cell lysates (Lysates) and concentrated culture supernatants (Sup) were subjected to Western blotting to detect M1 protein. The expression levels of M1 in the Osaka(3P+NP)-infected cells were significantly higher than those in the Osaka164- or Norway3487-infected cells at 9 and 12 h postinfection ($P < 0.05$), whereas no significant differences in the levels of released virus particles were observed among these virus groups.

N340K/PB1 I667T, indicating that these mutations (PB2 N340K or V649I and PB1 I667T), in concert with HA, NA, and NS derived from Norway3487, contribute to high virulence in mice.

DISCUSSION

Here, we demonstrated that HA is responsible for the increased pathogenicity of Norway3487, which was isolated from a fatal case

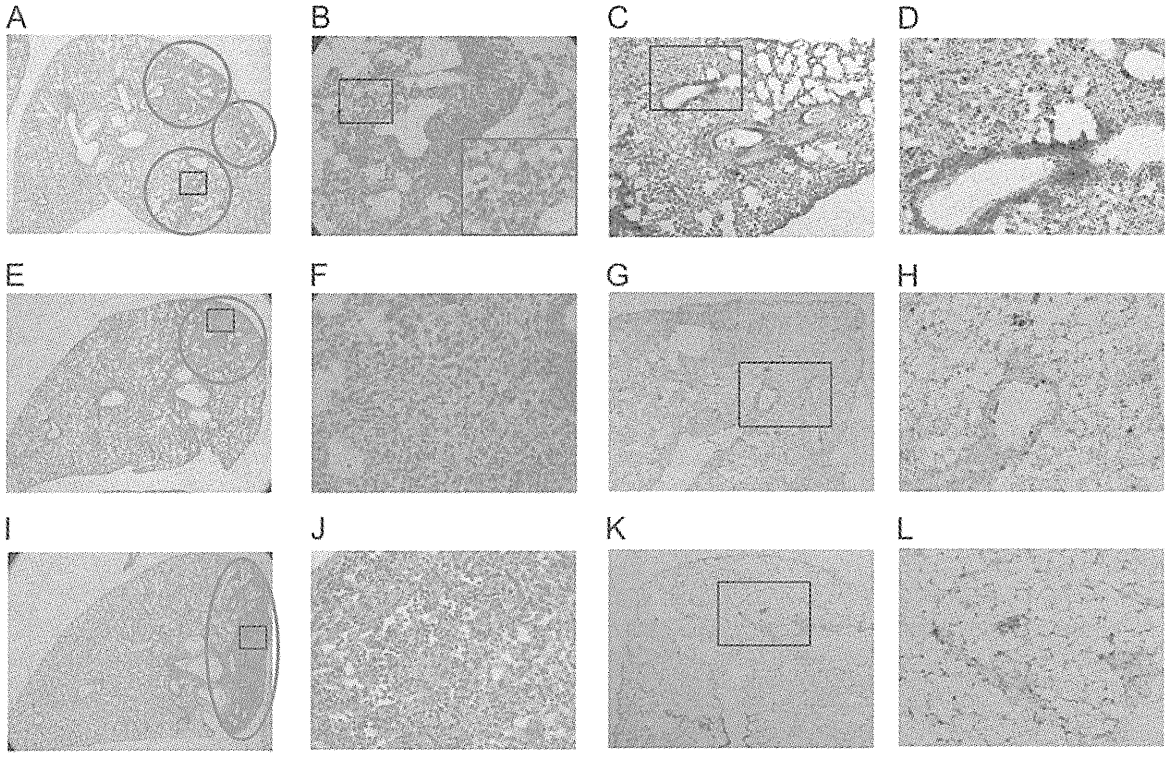

FIG 6 Pathological findings in mice infected with Osaka164, Norway3487, or Osaka(3P+NP). The images represent the lungs of mice infected with Osaka(3P+NP) (A to D), Norway3487 (E toH), or Osaka164 (I to L). (A, E, and I) Images of the lungs at low magnification are shown. The blue circles indicate the lesions. (B) Magnified view of the boxed area in panel A. Infiltration of neutrophils was obvious at 6 dpi and is indicated by red arrowheads. (F and J) Magnified views of the boxed areas in panels E and I. The lungs of mice infected with Norway3487 (F) or Osaka164 (J) exhibited lesions that included mononuclear cells, neutrophils, and regenerated epithelial cells. (C, G, and K) Immunostaining of lungs infected with Osaka(3P+NP) (C and D), Norway3487 (G and H), and Osaka164 (H and L) at 8 dpi at low magnification is shown. (D, H, and L) Magnified views of the boxed areas in panels C, G, and K, respectively. (D) Many viral antigen-positive cells (brown pigment) can be seen in the Osaka(3P+NP)-infected lungs, whereas few viral antigen-positive cells were present in lungs infected with Norway3487 (H) or Osaka164 (L).

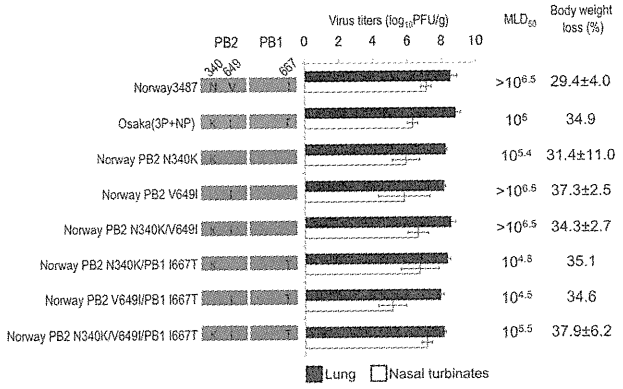

FIG 8 Characterization of mutant viruses in mice. Mice were intranasally inoculated with 10^4 PFU of Norway3487 and point mutant viruses. Three mice per group were euthanized at 3 dpi, and virus titers in the lungs (■) and nasal turbinates (□) were determined by using plaque assays in MDCK cells. The results are expressed as mean titers ± standard deviations (SD). MLD_{50} values were calculated by observing mice infected with 10^4, 10^5, or 10^6 PFU of Norway3487 or the point mutant viruses. The mean maximum body weight losses (%) ± standard deviations (SD) shown are for mice that were infected with 10^5 PFU.

and exhibited high virulence in mice. HA is critical for the host range restriction and pathogenicity of influenza viruses (3, 23–26). Generally, binding specificities to avian- or human-type receptors are determined by specific amino acids in HA (27, 28). For A(H1N1)pdm09 viruses, we and others have demonstrated that an Asp-to-Gly change at position 222 (H1 numbering) of HA, which confers avian-type receptor-binding specificity (15–19), results in enhanced virulence in mouse and nonhuman primate models (19–21, 34). In agreement with these previous findings (19–21), we found that Norway3487, which was the most pathogenic of the viruses tested in mice, possesses Gly at position 222 of HA (Table 1), whereas Osaka164 does not, thereby explaining the difference in virulence in mice between these two viruses. In addition, we tested the effect of the NS gene, which encodes the interferon (IFN) antagonist NS1 protein, on the interferon response because there are two amino acid differences between the NS1 of Norway3487 and that of Osaka164. The levels of IFN-β mRNA were similar among Norway3487-, Osaka164-, and Norway(NS)-infected cells (data not shown), suggesting that Norway3487 NS1 does not contribute to or offers a limited contribution to the pathogenicity of viruses.

Interestingly, we found that a reassortant virus, Osaka(3P+NP), possessing the polymerase complex of Osaka164 and its HA, NA, and NS genes from Norway3487, was more pathogenic in mice than was the parental Norway3487 virus (Table 2). Although there was no significant difference between the virus titers in the lungs of Norway3487 and Osaka(3P+NP) at 9 dpi, viral antigen-positive cells in the lungs of mice infected with Osaka(3P+NP) were more prevalent than in mice infected with the parental Norway3487 and Osaka164 viruses (Fig. 6). Our *in vitro* study demonstrated that the expression levels of viral protein in the Osaka(3P+NP)-infected cells were significantly higher than those in the Norway3487- or Osaka164-infected cells (Fig. 7), and this feature may contribute to the high prevalence of viral antigen-positive cells in the Osaka(3P+NP)-infected mouse lungs (Fig. 6). Therefore, it is highly possible that the increased and/or sustained expression of viral proteins in the lungs of the infected mice may contribute to enhanced immune responses (e.g., prolonged neutrophil accumulation and inflammatory responses) in the lungs, resulting in higher pathogenicity.

We further identified that Lys or Ile at position 340 or 649 of PB2, respectively, and Thr at position 667 of PB1 contribute to this high virulence of Osaka(3P+NP) in mice even though there was no marked difference in replication efficiencies among the three viruses (Fig. 8). Positions 667 in PB1 and 649 in PB2 are located in the interaction site between PB2 and PB1 (29–31), and position 340 in PB2 is located in the cap binding domain (31, 32). Additionally, viruses that possess both PB2-649I and PB1-667T are classified in clade 4 of the A(H1N1)pdm09 viruses (33). Of note, no viruses possessing only one of these two mutations has yet been found, indicating that these mutations might cooperate and provide an advantage in terms of stability or survival for viruses over the presence of either mutation alone. Since these amino acid differences had no effect on viral replicative ability *in vitro* or *in vivo* (Fig. 5, Fig. 8, and Table 3), we can hypothesize that the increased virulence of Osaka(3P+NP) might be attributed to other events, such as aberrant immune responses to infection with this virus. Further study is needed to assess the mechanistic role of these amino acids in the pathogenicity of A(H1N1)pdm09 viruses.

While most individuals infected with A(H1N1)pdm09 virus do not experience severe symptoms and recover without the need for hospitalization, this study demonstrates the risk of enhanced virulence as a result of reassortment. It is therefore imperative that we continue to monitor A(H1N1)pdm09 viruses to manage the risk associated with the emergence of more pathogenic strains.

ACKNOWLEDGMENTS

We thank Shinji Watanabe, Satoshi Fukuyama, Shinya Yamada, and Saori Sakabe for fruitful discussions. We also thank Susan Watson for editing the manuscript.

This work was supported by a Grant-in-Aid for Specially Promoted Research by the Japan Initiative for the Global Research Network on Infectious Diseases from the Ministry of Education, Culture, Sports, Science, and Technology, Japan, by grants-in-aid from the Ministry of Health, Labor, and Welfare, Japan, by ERATO (Japan Science and Technology Agency), by National Institute of Allergy and Infectious Diseases Public Health Service research grants, and by an NIAID-funded Center for Research on Influenza Pathogenesis (CRIP; HHSN266200700010C). R.U. is supported by JSPS Research Fellowships for young scientists.

REFERENCES

1. Eurosurveillance Editorial Team. 2009. Pandemic alert level 6: scientific criteria for an influenza pandemic fulfilled. Euro Surveill. 14:19237. http://www.eurosurveillance.org/ViewArticle.aspx?ArticleId=19237.
2. Fraser C, Donnelly CA, Cauchemez S, Hanage WP, Van Kerkhove MD, Hollingsworth TD, Griffin J, Baggaley RF, Jenkins HE, Lyons EJ, Jombart T, Hinsley WR, Grassly NC, Balloux F, Ghani AC, Ferguson NM, Rambaut A, Pybus OG, Lopez-Gatell H, Alpuche-Aranda CM, Chapela IB, Zavala EP, Guevara DM, Checchi F, Garcia E, Hugonnet S, Roth C. 2009. Pandemic potential of a strain of influenza A (H1N1): early findings. Science 324:1557–1561.
3. Garten RJ, Davis CT, Russell CA, Shu B, Lindstrom S, Balish A, Sessions WM, Xu X, Skepner E, Deyde V, Okomo-Adhiambo M, Gubareva L, Barnes J, Smith CB, Emery SL, Hillman MJ, Rivailler P, Smagala J, de Graaf M, Burke DF, Fouchier RA, Pappas C, Alpuche-Aranda CM, Lopez-Gatell H, Olivera H, Lopez I, Myers CA, Faix D, Blair PJ, Yu C, Keene KM, Dotson PD, Jr, Boxrud D, Sambol AR, Abid SH, ST George K, Bannerman T, Moore AL, Stringer DJ, Blevins P, Demmler-Harrison GJ, Ginsberg M, Kriner P, Waterman S, Smole S, Guevara HF, Belongia EA, Clark PA, Beatrice ST, Donis R, Katz J,

Finelli L, Bridges CB, Shaw M, Jernigan DB, Uyeki TM, Smith DJ, Klimov AI, Cox NJ. 2009. Antigenic and genetic characteristics of swine-origin 2009 A(H1N1) influenza viruses circulating in humans. Science 325:197–201.

4. Bautista E, Chotpitayasunondh T, Gao Z, Harper SA, Shaw M, Uyeki TM, Zaki SR, Hayden FG, Hui DS, Kettner JD, Kumar A, Lim M, Shindo N, Penn C, Nicholson KG. 2010. Clinical aspects of pandemic 2009 influenza A (H1N1) virus infection. N. Engl. J. Med. 362:1708–1719.
5. Jain S, Kamimoto L, Bramley AM, Schmitz AM, Benoit SR, Louie J, Sugerman DE, Druckenmiller JK, Ritger KA, Chugh R, Jasuja S, Deutscher M, Chen S, Walker JD, Duchin JS, Lett S, Soliva S, Wells EV, Swerdlow D, Uyeki TM, Fiore AE, Olsen SJ, Fry AM, Bridges CB, Finelli L. 2009. Hospitalized patients with 2009 H1N1 influenza in the United States, April-June 2009. N. Engl. J. Med. 361:1935–1944.
6. Kumar A, Zarychanski R, Pinto R, Cook DJ, Marshall J, Lacroix J, Stelfox T, Bagshaw S, Choong K, Lamontagne F, Turgeon AF, Lapinsky S, Ahern SP, Smith O, Siddiqui F, Jouvet P, Khwaja K, McIntyre L, Menon K, Hutchison J, Hornstein D, Joffe A, Lauzier F, Singh J, Karachi T, Wiebe K, Olafson K, Ramsey C, Sharma S, Dodek P, Meade M, Hall R, Fowler RA. 2009. Critically ill patients with 2009 influenza A(H1N1) infection in Canada. JAMA 302:1872–1879.
7. Louie JK, Acosta M, Winter K, Jean C, Gavali S, Schechter R, Vugia D, Harriman K, Matyas B, Glaser CA, Samuel MC, Rosenberg J, Talarico J, Hatch D, California Pandemic (H1N1) Working Group. 2009. Factors associated with death or hospitalization due to pandemic 2009 influenza A(H1N1) infection in California. JAMA 302:1896–1902.
8. Peiris JS, Poon LL, Guan Y. 2009. Emergence of a novel swine-origin influenza A virus (S-OIV) H1N1 virus in humans. J. Clin. Virol. 45:169–173.
9. Vaillant L, La Ruche G, Tarantola A, Barboza P. 2009. Epidemiology of fatal cases associated with pandemic H1N1 influenza 2009. Euro Surveill. 14:19309. http://www.eurosurveillance.org/ViewArticle.aspx?ArticleId=19309.
10. Gabriel G, Abram M, Keiner B, Wagner R, Klenk HD, Stech J. 2007. Differential polymerase activity in avian and mammalian cells determines host range of influenza virus. J. Virol. 81:9601–9604.
11. Hatta M, Gao P, Halfmann P, Kawaoka Y. 2001. Molecular basis for high virulence of Hong Kong H5N1 influenza A viruses. Science 293:1840–1842.
12. Li Z, Chen H, Jiao P, Deng G, Tian G, Li Y, Hoffmann E, Webster RG, Matsuoka Y, Yu K. 2005. Molecular basis of replication of duck H5N1 influenza viruses in a mammalian mouse model. J. Virol. 79:12058–12064.
13. Mehle A, Doudna JA. 2009. Adaptive strategies of the influenza virus polymerase for replication in humans. Proc. Natl. Acad. Sci. U. S. A. 106:21312–21316.
14. Yamada S, Hatta M, Staker BL, Watanabe S, Imai M, Shinya K, Sakai-Tagawa Y, Ito M, Ozawa M, Watanabe T, Sakabe S, Li C, Kim JH, Myler PJ, Phan I, Raymond A, Smith E, Stacy R, Nidom CA, Lank SM, Wiseman RW, Bimber BN, O'Connor DH, Neumann G, Stewart LJ, Kawaoka Y. 2010. Biological and structural characterization of a host-adapting amino acid in influenza virus. PLoS Pathog. 6:e1001034. doi:10.1371/journal.ppat.1001034.
15. Abed Y, Pizzorno A, Hamelin ME, Leung A, Joubert P, Couture C, Kobasa D, Boivin G. 2011. The 2009 pandemic H1N1 D222G hemagglutinin mutation alters receptor specificity and increases virulence in mice but not in ferrets. J. Infect. Dis. 204:1008–1016.
16. Belser JA, Jayaraman A, Raman R, Pappas C, Zeng H, Cox NJ, Katz JM, Sasisekharan R, Tumpey TM. 2011. Effect of D222G mutation in the hemagglutinin protein on receptor binding, pathogenesis and transmissibility of the 2009 pandemic H1N1 influenza virus. PLoS One 6:e25091. doi:10.1371/journal.pone.0025091.
17. Chutinimitkul S, Herfst S, Steel J, Lowen AC, Ye J, van Riel D, Schrauwen EJ, Bestebroer TM, Koel B, Burke DF, Sutherland-Cash KH, Whittleston CS, Russell CA, Wales DJ, Smith DJ, Jonges M, Meijer A, Koopmans M, Rimmelzwaan GF, Kuiken T, Osterhaus AD, Garcia-Sastre A, Perez DR, Fouchier RA. 2010. Virulence-associated substitution D222G in the hemagglutinin of 2009 pandemic influenza A(H1N1) virus affects receptor binding. J. Virol. 84:11802–11813.
18. Liu Y, Childs RA, Matrosovich T, Wharton S, Palma AS, Chai W, Daniels R, Gregory V, Uhlendorff J, Kiso M, Klenk HD, Hay A, Feizi T, Matrosovich M. 2010. Altered receptor specificity and cell tropism of D222G hemagglutinin mutants isolated from fatal cases of pandemic A(H1N1) 2009 influenza virus. J. Virol. 84:12069–12074.
19. Watanabe T, Shinya K, Watanabe S, Imai M, Hatta M, Li CJ, Wolter BF, Neumann G, Hanson A, Ozawa M, Yamada S, Imai H, Sakabe S, Takano R, Iwatsuki-Horimoto K, Kiso M, Ito M, Fukuyama S, Kawakami E, Gorai T, Simmons HA, Schenkman D, Brunner K, Capuano SV, Weinfurter JT, Nishio W, Maniwa Y, Igarashi T, Makino A, Travanty EA, Wang JR, Kilander A, Dudman SG, Suresh M, Mason RJ, Hungnes O, Friedrich TC, Kawaoka Y. 2011. Avian-type receptor-binding ability can increase influenza virus pathogenicity in macaques. J. Virol. 85:13195–13203.
20. Sakabe S, Ozawa M, Takano R, Iwastuki-Horimoto K, Kawaoka Y. 2011. Mutations in PA, NP, and HA of a pandemic (H1N1) 2009 influenza virus contribute to its adaptation to mice. Virus Res. 158:124–129.
21. Xu L, Bao L, Lv Q, Deng W, Ma Y, Li F, Zhan L, Zhu H, Ma C, Qin C. 2010. A single-amino-acid substitution in the HA protein changes the replication and pathogenicity of the 2009 pandemic A (H1N1) influenza viruses in vitro and in vivo. Virol. J. 7:325. doi:10.1186/1743-422X-7-325.
22. Neumann G, Watanabe T, Ito H, Watanabe S, Goto H, Gao P, Hughes M, Perez DR, Donis R, Hoffmann E, Hobom G, Kawaoka Y. 1999. Generation of influenza A viruses entirely from cloned cDNAs. Proc. Natl. Acad. Sci. U. S. A. 96:9345–9350.
23. Couceiro JN, Paulson JC, Baum LG. 1993. Influenza virus strains selectively recognize sialyloligosaccharides on human respiratory epithelium: the role of the host cell in selection of hemagglutinin receptor specificity. Virus Res. 29:155–165.
24. Neumann G, Kawaoka Y. 2006. Host range restriction and pathogenicity in the context of influenza pandemic. Emerg. Infect. Dis. 12:881–886.
25. Rogers GN, Paulson JC. 1983. Receptor determinants of human and animal influenza virus isolates: differences in receptor specificity of the H3 hemagglutinin based on species of origin. Virology 127:361–373.
26. Rogers GN, Paulson JC, Daniels RS, Skehel JJ, Wilson IA, Wiley DC. 1983. Single amino acid substitutions in influenza haemagglutinin change receptor binding specificity. Nature 304:76–78.
27. Matrosovich M, Tuzikov A, Bovin N, Gambaryan A, Klimov A, Castrucci MR, Donatelli I, Kawaoka Y. 2000. Early alterations of the receptor-binding properties of H1, H2, and H3 avian influenza virus hemagglutinins after their introduction into mammals. J. Virol. 74:8502–8512.
28. Rogers GN, Pritchett TJ, Lane JL, Paulson JC. 1983. Differential sensitivity of human, avian, and equine influenza A viruses to a glycoprotein inhibitor of infection: selection of receptor specific variants. Virology 131:394–408.
29. Area E, Martin-Benito J, Gastaminza P, Torreira E, Valpuesta JM, Carrascosa JL, Ortin J. 2004. 3D structure of the influenza virus polymerase complex: localization of subunit domains. Proc. Natl. Acad. Sci. U. S. A. 101:308–313.
30. Poole E, Elton D, Medcalf L, Digard P. 2004. Functional domains of the influenza A virus PB2 protein: identification of NP- and PB1-binding sites. Virology 321:120–133.
31. Sugiyama K, Obayashi E, Kawaguchi A, Suzuki Y, Tame JR, Nagata K, Park SY. 2009. Structural insight into the essential PB1-PB2 subunit contact of the influenza virus RNA polymerase. EMBO J. 28:1803–1811.
32. Guilligay D, Tarendeau F, Resa-Infante P, Coloma R, Crepin T, Sehr P, Lewis J, Ruigrok RW, Ortin J, Hart DJ, Cusack S. 2008. The structural basis for cap binding by influenza virus polymerase subunit PB2. Nat. Struct. Mol. Biol. 15:500–506.
33. Nelson M, Spiro D, Wentworth D, Beck E, Fan J, Ghedin E, Halpin R, Bera J, Hine E, Proudfoot K, Stockwell T, Lin X, Griesemer S, Kumar S, Bose M, Viboud C, Holmes E, Henrickson K. 2009. The early diversification of influenza A/H1N1pdm. PLoS Curr. 1:RRN1126. doi:10.1371/currents.RRN1126.
34. Stevens J, Blixt O, Glaser L, Taubenberger JK, Palese P, Paulson JC, Wilson IA. 2006. Glycan microarray analysis of the hemagglutinins from modern and pandemic influenza viruses reveals different receptor specificities. J. Mol. Biol. 355:1143–1155.

Journal of Virology

Competitive Incorporation of Homologous Gene Segments of Influenza A Virus into Virions

Arisa Inagaki, Hideo Goto, Satoshi Kakugawa, Makoto Ozawa and Yoshihiro Kawaoka

***J. Virol.* 2012, 86(18):10200. DOI: 10.1128/JVI.01204-12.**
Published Ahead of Print 27 June 2012.

JVI
Journals.ASM.org

Competitive Incorporation of Homologous Gene Segments of Influenza A Virus into Virions

Arisa Inagaki,[a] Hideo Goto,[a] Satoshi Kakugawa,[a] Makoto Ozawa,[b,c] and Yoshihiro Kawaoka[a,d,e,f]

Division of Virology, Department of Microbiology and Immunology, Institute of Medical Science, University of Tokyo, Shirokanedai, Minato-ku, Tokyo, Japan[a]; Laboratory of Animal Hygiene, Joint Faculty of Veterinary Medicine, Kagoshima University, Kagoshima, Japan[b]; Transboundary Animal Diseases Center, Joint Faculty of Veterinary Medicine, Kagoshima University, Kagoshima, Japan[c]; Department of Special Pathogens, International Research Center for Infectious Diseases, Institute of Medical Science, University of Tokyo, Shirokanedai, Minato-ku, Tokyo, Japan[d]; Department of Pathobiological Sciences, School of Veterinary Medicine, University of Wisconsin, Madison, Wisconsin, USA[e]; and ERATO Infection-Induced Host Responses Project, Japan Science and Technology Agency, Saitama, Japan[f]

By using two reporter protein-encoding virus-like RNAs derived from identical viral RNA (vRNA) segments, we assessed their incorporation efficiency into single progeny virions. Most plaques formed by the recombinant viruses that were generated in cells positive for both reporter genes expressed only one or the other protein. These results suggest that two virus-like RNAs encoding different reporter proteins compete for incorporation into virions, and individual influenza virions incorporate single, but not multiple, copies of homologous vRNA segments.

The influenza A virus genome is segmented into eight negative-sense RNAs. Although this segmented genome allows viruses to evolve rapidly through gene reassortment, all of the eight viral RNA (vRNA) segments need to be introduced into a cell for the viruses to be infectious (18). In virions, eight kinds of RNA molecules were detected at a comparable molar ratio in purified viruses (17). Previously, we used electron microscopy to show that eight rods, which were most likely vRNA-associated ribonucleoprotein complexes (RNPs), were packed in budding virions in an orderly fashion (12). Further, the three-dimensional structure of the RNPs revealed that the eight rod-like structures were of different lengths and well organized but asymmetrically arranged in progeny virions (2, 13). These findings suggest that the individual influenza virions incorporate eight vRNA segments; however, it remains unclear whether the eight rods correspond to the eight genetically distinct vRNA segments (i.e., the eight distinct vRNA segments are present in individual virions) or some rods are genetically identical (i.e., multiple copies of homologous vRNA segments are packaged in individual virions and the eight vRNA segments are maintained as virus populations).

We therefore attempted to assess the incorporation efficiency of two reporter protein-encoding virus-like RNAs derived from identical vRNA segments. We (3, 4, 10, 13–15) and others (1, 5–9) have reported that the noncoding and coding sequences at the 3′ and 5′ ends of each vRNA segment are essential for efficient segment incorporation into virions. According to these findings, we constructed a plasmid encoding two RNA polymerase I promoter-driven transcription cassettes for virus-like RNA expression (Fig. 1A to C). One transcription cassette produces negative-sense RNA containing the 3′ noncoding sequence of the neuraminidase (NA) vRNA segment, 183 nucleotides of the 3′ coding sequence of the NA vRNA segment, the open reading frame of green fluorescent protein (GFP; Clontech), 157 nucleotides of the 5′ coding sequence of the NA vRNA segment, and the 5′ noncoding sequence of the NA vRNA segment (Fig. 1A). Another cassette produces the same virus-like RNA except that the GFP reporter gene was replaced with the gene encoding DsRed-monomer fluorescent protein (DsRed; Clontech) (Fig. 1B). The length of the coding sequence at each end is required for efficient incorporation of the NA vRNA segment (4). To ensure that the two virus-like vRNAs encoding different reporter proteins were produced in the same cells, we constructed plasmids containing the two transcription cassettes. Further, to eliminate any effect of gene order in the plasmid on the expression level of the virus-like RNAs, we prepared two types of plasmids containing the two transcription cassettes in a different order (Fig. 1C).

To confirm that the resultant "tandem" reporter plasmids indeed produced both GFP- and DsRed-encoding virus-like RNAs in cells, 293T cells were transfected with the plasmids together with four protein plasmids for the expression of the A/WSN/33 (H1N1, WSN) viral polymerase subunits (PB2, PB1, and PA) and nucleoprotein NP, which are required for vRNA transcription and replication (18). At 24 h posttransfection, GFP- and/or DsRed-expressing cells were counted under a fluorescence microscope. Approximately half (45.7%) of the fluorescent protein-positive cells expressed both GFP and DsRed (Fig. 1D).

Next, to assess the incorporation efficiency of the two virus-like NA vRNA segments encoding the reporter proteins into single progeny virions, we generated WSN-based NA-knockout recombinant influenza viruses by using reverse genetics (11) with the tandem reporter plasmids instead of a plasmid for the expression of the intact NA vRNA. At 24 h posttransfection, culture supernatants were clarified and subjected to plaque assays in Madin-Darby canine kidney (MDCK) cells. These NA-knockout viruses formed small plaques in MDCK cells as described previously (4); most of the plaques expressed fluorescent proteins at 24 to 48 h postinfection (data not shown). We then counted the GFP- and/or DsRed-positive plaques. Most of the plaques expressed only either GFP (59.3%) or DsRed (39.1%) (Fig. 1E); only a small portion (1.6%) of the plaques was positive for both GFP and

Received 13 May 2012 Accepted 20 June 2012
Published ahead of print 27 June 2012
Address correspondence to Yoshihiro Kawaoka, kawaokay@svm.vetmed.wisc.edu.

doi:10.1128/JVI.01204-12

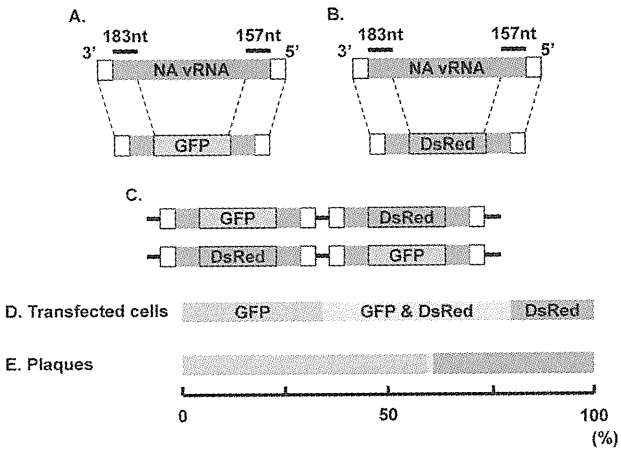

FIG 1 Competitive incorporation of the NA vRNA segment into virions. (A to C) Schematic diagram of influenza virus-like RNA constructs. Transcription cassettes for GFP (green bar in panel A) and DsRed (red bar in panel B) genes flanked by the 3′ and 5′ noncoding (white bars) and coding (gray bars) sequences of the NA vRNA segment were cloned into RNA polymerase I promoter-driven plasmids for the expression of influenza virus-like RNA (11) in different configurations (panel C). (D) Ratio of fluorescent protein-expressing plasmid-transfected cells. 293T cells were transfected with NA vRNA segment-derived tandem reporter plasmids together with protein expression plasmids required for vRNA transcription and replication. At 24 h posttransfection, cells positive for GFP only (green bar), DsRed only (red bar), and both GFP and DsRed (yellow) were counted under a fluorescence microscope. Mean ratios of each cell population calculated from three independent experiments are shown. (E) Ratio of fluorescent protein-expressing virus-formed plaques. MDCK cells were infected with NA-knockout viruses generated in cells that were transfected with an NA vRNA segment-derived tandem reporter plasmid, and plaque assays were performed. At 24 h postinfection, plaques positive for GFP only (green bar), DsRed only (red bar), and both GFP and DsRed (yellow) were counted under a fluorescence microscope. Mean ratios of each plaque population calculated from three independent experiments are shown.

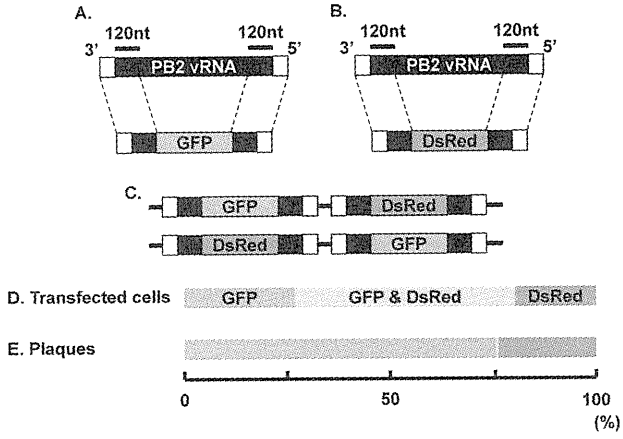

FIG 2 Competitive incorporation of the PB2 vRNA segment into virions. (A to C) Schematic diagram of influenza virus-like RNA constructs. Transcription cassettes for GFP (green bar in panel A) and DsRed (red bar in panel B) genes flanked by the 3′ and 5′ noncoding (white bars) and coding (black bars) sequences of the PB2 vRNA segment were cloned into RNA polymerase I promoter-driven plasmids in different configurations (panel C). (D) Ratio of fluorescent protein-expressing plasmid-transfected cells. 293T cells were transfected with PB2 vRNA segment-derived tandem reporter plasmids together with protein expression plasmids required for vRNA transcription and replication. At 24 h posttransfection, cells positive for GFP only (green bar), DsRed only (red bar), and both GFP and DsRed (yellow) were counted under a fluorescence microscope. Mean ratios of each cell population calculated from three independent experiments are shown. (E) Ratio of fluorescent protein-expressing virus-formed plaques. PB2 protein-expressing MDCK cells were infected with PB2-knockout viruses generated in cells that were transfected with a PB2 vRNA segment-derived tandem reporter plasmid, and plaque assays were performed. At 24 h postinfection, plaques positive for GFP only (green bar), DsRed only (red bar), and both GFP and DsRed (yellow) were counted under a fluorescence microscope. Mean ratios of each plaque population calculated from three independent experiments are shown.

DsRed (Fig. 1E). These results suggest that the two reporter virus-like RNAs competed for incorporation into individual virions.

The competitive effect of the two reporter virus-like RNAs was also assessed by using PB2 vRNA segment-based virus-like RNAs. We constructed tandem reporter plasmids for the recombinant PB2 vRNA segment (Fig. 2A to C). These plasmids encoded the 3′ and 5′ ends of the PB2 vRNA segment including 120 nucleotides of each coding sequence, which were required for efficient incorporation of the PB2 vRNA segment (15). The expression of both GFP- and DsRed-encoding virus-like RNAs in cells transfected with the tandem reporter plasmids was confirmed as described above. Similar to the results with the NA vRNA segment-based plasmids, approximately half (53.5%) of the transfected cells expressed GFP and DsRed (Fig. 2D). By using these tandem reporter plasmids instead of an intact PB2 vRNA-expressing plasmid, we generated PB2-knockout viruses by means of reverse genetics. We then counted the GFP- and/or DsRed-positive plaques formed by the transfectant viruses in PB2 protein-expressing MDCK cells that were established by using a retrovirus vector as described previously (16). Like the NA-knockout viruses, these PB2-knockout viruses mainly formed plaques expressing only either GFP (75.6%) or DsRed (23.8%); only a limited portion (0.6%) of the plaques expressed both GFP and DsRed (Fig. 2E). These results indicate that, as with the NA segment, only a single PB2 segment is incorporated into virions.

Here, we demonstrated that two virus-like RNAs derived from identical vRNA segments competed for incorporation into progeny viruses. Although half of the cells transfected with plasmids for virus generation were positive for two reporter proteins (Fig. 1D and 2D), most of the plaques formed by the transfectant viruses were positive for only one or the other protein (Fig. 1E and 2E). These findings suggest that individual influenza virions incorporate single, not multiple, copies of homologous vRNA segments, that is, the eight distinct vRNA segments required for virus replication are present in individual virions.

ACKNOWLEDGMENTS

We thank Susan Watson for editing the manuscript.

This work was supported by ERATO (Japan Science and Technology Agency), by a grant-in-aid for Specially Promoted Research from the Ministries of Education, Culture, Sport, Science, and Technology, by a grant-in-aid from Health, Labor, and Welfare of Japan, by a Contract Research Fund for the Program of Founding Research Centers for Emerging and Reemerging Infectious Diseases, and by National Institute of Allergy and Infectious Diseases Public Health Service research grants.

REFERENCES

1. Dos Santos Afonso E, Escriou N, Leclercq I, van der Werf S, Naffakh N. 2005. The generation of recombinant influenza A viruses expressing a PB2 fusion protein requires the conservation of a packaging signal overlapping the coding and noncoding regions at the 5′ end of the PB2 segment. Virology 341:34–46.

2. **Fournier E, et al.** 2012. A supramolecular assembly formed by influenza A virus genomic RNA segments. Nucleic Acids Res. **40**:2197–2209.
3. **Fujii K, et al.** 2005. Importance of both the coding and the segment-specific noncoding regions of the influenza A virus NS segment for its efficient incorporation into virions. J. Virol. **79**:3766–3774.
4. **Fujii Y, Goto H, Watanabe T, Yoshida T, Kawaoka Y.** 2003. Selective incorporation of influenza virus RNA segments into virions. Proc. Natl. Acad. Sci. U. S. A. **100**:2002–2007.
5. **Gog JR, et al.** 2007. Codon conservation in the influenza A virus genome defines RNA packaging signals. Nucleic Acids Res. **35**:1897–1907.
6. **Liang Y, Hong Y, Parslow TG.** 2005. *cis*-Acting packaging signals in the influenza virus PB1, PB2, and PA genomic RNA segments. J. Virol. **79**: 10348–10355.
7. **Liang Y, Huang T, Ly H, Parslow TG, Liang Y.** 2008. Mutational analyses of packaging signals in influenza virus PA, PB1, and PB2 genomic RNA segments. J. Virol. **82**:229–236.
8. **Marsh GA, Hatami R, Palese P.** 2007. Specific residues of the influenza A virus hemagglutinin viral RNA are important for efficient packaging into budding virions. J. Virol. **81**:9727–9736.
9. **Marsh GA, Rabadan R, Levine AJ, Palese P.** 2008. Highly conserved regions of influenza a virus polymerase gene segments are critical for efficient viral RNA packaging. J. Virol. **82**:2295–2304.
10. **Muramoto Y, et al.** 2006. Hierarchy among viral RNA (vRNA) segments in their role in vRNA incorporation into influenza A virions. J. Virol. **80**:2318–2325.
11. **Neumann G, et al.** 1999. Generation of influenza A viruses entirely from cloned cDNAs. Proc. Natl. Acad. Sci. U. S. A. **96**:9345–9350.
12. **Noda T, et al.** 2006. Architecture of ribonucleoprotein complexes in influenza A virus particles. Nature **439**:490–492.
13. **Noda T, et al.** 2012. Three-dimensional analysis of ribonucleoprotein complexes in influenza A virus. Nat. Commun. **3**:639.
14. **Ozawa M, et al.** 2007. Contributions of two nuclear localization signals of influenza A virus nucleoprotein to viral replication. J. Virol. **81**:30–41.
15. **Ozawa M, et al.** 2009. Nucleotide sequence requirements at the 5′ end of the influenza A virus M RNA segment for efficient virus replication. J. Virol. **83**:3384–3388.
16. **Ozawa M, et al.** 2011. Replication-incompetent influenza A viruses that stably express a foreign gene. J. Gen. Virol. **92**:2879–2888.
17. **Palese P, Schulman JL.** 1976. Differences in RNA patterns of influenza A viruses. J. Virol. **17**:876–884.
18. **Palese P, Shaw ML.** 2007. Orthomyxoviridae: the viruses and their replication, p 1647–1689. *In* Knipe DM, Howley PM (ed), Fields virology, 5th ed. Lippincott-Raven Publishers, Philadelphia, PA.

OPEN ACCESS Freely available online

PLOS ONE

High Yield Production of Influenza Virus in Madin Darby Canine Kidney (MDCK) Cells with Stable Knockdown of IRF7

Itsuki Hamamoto[1], Hiroshi Takaku[2], Masato Tashiro[1], Norio Yamamoto[1,3]*

1 Laboratory of Cell-based Vaccine Development, Influenza Virus Research Center, National Institute of Infectious Diseases, Musashimurayama-shi, Tokyo, Japan, **2** Department of Life and Environmental Science, Chiba Institute of Technology, Narashino-shi, Chiba, Japan, **3** Department of General Medicine, Juntendo University School of Medicine, Bunkyo-ku, Tokyo, Japan

Abstract

Influenza is a serious public health problem that causes a contagious respiratory disease. Vaccination is the most effective strategy to reduce transmission and prevent influenza. In recent years, cell-based vaccines have been developed with continuous cell lines such as Madin-Darby canine kidney (MDCK) and Vero. However, wild-type influenza and egg-based vaccine seed viruses will not grow efficiently in these cell lines. Therefore, improvement of virus growth is strongly required for development of vaccine seed viruses and cell-based influenza vaccine production. The aim of our research is to develop novel MDCK cells supporting highly efficient propagation of influenza virus in order to expand the capacity of vaccine production. In this study, we screened a human siRNA library that involves 78 target molecules relating to three major type I interferon (IFN) pathways to identify genes that when knocked down by siRNA lead to enhanced production of influenza virus A/Puerto Rico/8/1934 in A549 cells. The siRNAs targeting 23 candidate genes were selected to undergo a second screening pass in MDCK cells. We examined the effects of knockdown of target genes on the viral production using newly designed siRNAs based on sequence analyses. Knockdown of the expression of a canine gene corresponding to human IRF7 by siRNA increased the efficiency of viral production in MDCK cells through an unknown process that includes the mechanisms other than inhibition of IFN-α/β induction. Furthermore, the viral yield greatly increased in MDCK cells stably transduced with the lentiviral vector for expression of short hairpin RNA against IRF7 compared with that in control MDCK cells. Therefore, we propose that modified MDCK cells with lower expression level of IRF7 could be useful not only for increasing the capacity of vaccine production but also facilitating the process of seed virus isolation from clinical specimens for manufacturing of vaccines.

Citation: Hamamoto I, Takaku H, Tashiro M, Yamamoto N (2013) High Yield Production of Influenza Virus in Madin Darby Canine Kidney (MDCK) Cells with Stable Knockdown of IRF7. PLoS ONE 8(3): e59892. doi:10.1371/journal.pone.0059892

Editor: Yi Guan, The University of Hong Kong, China

Received September 10, 2012; **Accepted** February 22, 2013; **Published** March 26, 2013

Funding: This work was supported by a Health Sciences Research Grant-in-Aid for Emerging and Re-emerging Infectious Diseases from the Ministry of Health, Labour and Welfare of Japan, and the Program for the Promotion of Fundamental Studies in Health Sciences of the National Institute of Biomedical Innovation of Japan. This study was also supported in part by a Grant-in-Aid (S1201013) from MEXT (Ministry of Education, Culture, Sports, Science and Technology) - Supported Program for the Strategic Research Foundation at Private Universities, 2012–2017. The funders had no role in study design, data collection and analysis, decision to publish, or preparation of the manuscript.

Competing Interests: The authors declare that they have a patent relating to material pertinent to this article. The technology of modified MDCK cells described in this manuscript was filed with the Japan Patent Office for a patent application (Composition for culturing cells, method for the preparation of influenza virus, and influenza virus, Japan patent application No. 2012093016, 16 April 2012). This does not alter the authors' adherence to all the PLOS ONE policies on sharing data and materials.

* E-mail: n-yama-5@nih.go.jp

Introduction

Influenza is a global public health issue that causes a serious illness with a high mortality rate. Vaccination is one of the most effective medical strategies to prevent influenza virus infection. The current egg-based technology for manufacturing influenza vaccine has been used since 1950s, but cell-based technology has been developed to produce more effective influenza vaccines in sufficient quantities in a shorter period of time. In recent years, two continuous cell lines have been approved by regulatory authorities to be used for the production of influenza vaccines: Madin Darby canine kidney (MDCK) cells and African green monkey kidney-derived Vero cells [1–5]. Human retina-derived cell line PER.C6 has also been shown useful for propagation of influenza viruses [6]. Although these cell lines produce notable yields of a wide variety of influenza viruses, attempts to develop novel cell lines with greater potentials have been made for more rapid preparation of influenza vaccines. A recent study demonstrated that the *siat7e*-expressing MDCK cells produce much more HA antigen than the parental MDCK cells [5]. The *siat7e*-expressing cells that proliferate in suspension would facilitate influenza virus productions [5].

Influenza viruses have been shown to be recognized by pattern-recognition receptors (PRRs), such as the Toll-like receptors 3 (TLR3) [7] and 7/8 (TLR7/8) [8], and retinoic acid-inducible gene (RIG-I)-like receptors (RLRs) [9]. Influenza viruses have evolved strategies to counteract cellular antiviral mechanisms, especially to circumvent the type I interferon (IFN-α/β) system which is a first line of defense against viral infections [10,11]. The mechanisms that underlie the induction of type I IFN genes have been extensively studied in the context of immunity to viruses.

Type I IFNs are known to be critical for inflammation [12] and play central roles in the activation of host antiviral responses to control virus infections [13,14]. Therefore, we hypothesized that it would be possible to obtain novel MDCK cells with greater potential to propagate influenza viruses by means of RNA-interference to inhibit the function of genes relating to IFN signaling.

In this study, we identified canine IRF7 as a target in order to establish modified MDCK cells which would be capable of producing higher yield of influenza A viruses. Knockdown of IRF7 with siRNA showed 3 to 4-fold enhancement of influenza A virus production. We also confirmed that MDCK cells with stable knockdown of IRF7 by short hairpin RNA (shRNA) showed 2 to 8-fold enhancement of influenza virus production. In conclusion, the modified MDCK cells with lower level of IRF7 expression may be useful for producing higher titers of influenza viruses. The novel MDCK cells will be beneficial for large-scale production of influenza vaccines in the manufacturing process. In addition, the established MDCK cells will be useful for isolation of influenza viruses from clinical specimens with a low viral load and efficient preparation of vaccine seed viruses in a shorter period.

Materials and Methods

Cells

A549 cells were purchased from Japanese Collection of Research Bioresources (JCRB; Osaka Japan). A549 cells were cultured in Dulbecco's modified Eagle's medium (DMEM; GIBCO, Carlsbad, CA) containing 10% fetal bovine serum (FBS; GIBCO, Carlsbad, CA) and 100 units/ml penicillin/streptomycin (GIBCO, Carlsbad, CA). MDCK (CCL-34) cells were purchased from American Type Culture Collection (ATCC; Rockville, MD). MDCK cells were cultured in Opti-Pro serum free medium (Opti-pro SFM; GIBCO, Carlsbad, CA) containing 4 mM L-Glutamine (GIBCO, Carlsbad, CA). All cells were cultured in a 5% CO_2 humidified incubator.

Viruses

Viruses used in this study were A/Puerto Rico/8/1934 (PR8; A(H1N1)), A/Narita/1/2009 (NR1; A(H1N1)pdm09), A/Victoria/361/2011 (VC361; A(H3N2)), and B/Florida/4/2006 (FL4; type B, Yamagata lineage). These viruses were propagated in MDCK cells. The virus titers were determined by 50% tissue culture infectious dose ($TCID_{50}$) assay or plaque assay.

siRNA Transfection, Virus Infection and RNA Extraction

The siRNA duplexes for A549 cells were selected from Silencer select siRNA library (Ambion, Austin, TX). The siRNA duplexes for MDCK cells were synthesized (Sigma-Aldrich, St. Louis, MO). The sequences of siRNA duplexes for MDCK cells were listed in Table 1. A549 cells were seeded on type I collagen coated 96-well plate. Three target-specific siRNAs (Silencer select siRNA library, Ambion, Austin, TX) or non-targeting negative control siRNA (Silencer Negative Control #1 siRNA, Ambion, Austin, TX) at a final concentration of 10 nM were transfected using transfection reagent (Lipofectamine RNAiMAX; Invitrogen, Carlsbad, CA) and incubated at 37°C for 48 h. For MDCK cells, the cells were seeded on 96-well plate and three target-specific siRNAs (Sigma-Aldrich, Inc., St. Louis, MO) or non-targeting negative control siRNA (Silencer Negative Control #1 siRNA, Ambion, Austin, TX) at a final concentration of 50 nM were transfected by siRNA transfection reagent (Lullaby; OZ Biosciences, France). Cells were washed with PBS three times and infected with influenza A virus at a MOI of 0.01 in Opti-Pro SFM in the presence of 2 μg/ml of trypsin acetylated (Sigma, Chemical Co., St. Louis, MO) at 34°C for 1 h. Then, cells were washed with PBS three times and incubated in Opti-Pro SFM supplemented with 2 μg/ml of trypsin acetylated at 37°C for 24 h. The viral RNA from tissue culture supernatant was mixed with the lysis buffer containing carrier RNA derived from uninfected A549 or MDCK cells and was extracted using MagMAX^{TM}-96 Blood RNA Isolation Kit (Ambion, Austin, TX) on King Fisher purification systems (Thermo Scientific, Cambridge, MA). The total RNA from cultured cells was extracted using RNeasy Mini Kit (Qiagen, Hilden, Germany) followed by DNase I (Qiagen, Hilden, Germany) treatment.

Plasmids

The pRetro-U6 vector was constructed by inserting a human U6 promoter amplified by PCR from genomic DNA into pMSCV-puro (Clontech, Mountain View, CA), from which DNA sequence between Nhe I and Xba I in the 3' LTR was deleted for generation of a self-inactivating virus. DNA fragments encoding the small hairpin RNAs were generated by PCR, digested with Bpi I, and ligated into pRetro-U6 between Bpi I sites downstream of the U6 promoter. The target sequences of shRNAs were as follows: shIRF7, 5'-CTGGGCAAATGCAAGGTCT-3'; shCtrl, 5'-GACTACACAAATCAGCGAT-3' (shCtrl targets LacZ). The shRNA expression cassettes were then transferred to pCS-BS, carrying a blasticidin S resistance gene expressed under the control of the elongation factor 1α promoter. The pCS-BS vector was constructed by replacing EGFP of the pCS-CDF-EG-

Table 1. Canis lupus familiaris siRNA used in this study.

Target Gene	Orientation	Sequences (5′ to 3′)
IRF7_1	Sense	CUGGGCAAAUGCAAGGUCUTT
IRF7_1	Anti-sense	AGACCUUGCAUUUGCCCAGTT
IRF7_2	Sense	GGCGCCUGGGCAAAUGCAATT
IRF7_2	Anti-sense	UUGCAUUUGCCCAGGCGCCTT
IRF7_3	Sense	CAGAGAAGCUGCUGCAGCATT
IRF7_3	Anti-sense	UGCUGCAGCAGCUUCUCUGTT
IRF3_1	Sense	GAUCUGAUUGCCUUCAUCATT
IRF3_1	Anti-sense	UGAUGAAGGCAAUCAGAUCTT
IRF3_2	Sense	GGCUCUUGGUGCCUGAUGATT
IRF3_2	Anti-sense	UCAUCAGGCACCAAGAGCCTT
IRF3_3	Sense	CAGACAGUCUCCUGCCCAATT
IRF3_3	Anti-sense	UUGGGCAGGAGACUGUCUGTT
MyD88_1	Sense	GGGCAAAUGCCUGAGCGUUTT
MyD88_1	Anti-sense	AACGCUCAGGCAUUUGCCCTT
MyD88_2	Sense	CAGACAAACUAUCGGCUGATT
MyD88_2	Anti-sense	UCAGCCGAUAGUUUGUCUGTT
MyD88_3	Sense	GCAUCACCAUGCUUGAUGATT
MyD88_3	Anti-sense	UCAUCAAGCAUGGUGAUGCTT
DDX58_1	Sense	CAAACUGUGUGCUUCUCUUTT
DDX58_1	Anti-sense	AAGAGAAGCACACAGUUUGTT
DDX58_2	Sense	GUGUUUCAGUUACCCAACATT
DDX58_2	Anti-sense	UGUUGGGUAACUGAAACACTT
DDX58_3	Sense	GAUCUGAUUGCCUUCAUCATT
DDX58_3	Anti-sense	UGAUGCAUUUAAAUCUGUCTT

doi:10.1371/journal.pone.0059892.t001

PRE vector (a kind gift from Dr. Hiroyuki Miyoshi, RIKEN, Tsukuba) with blasticidin S resistance gene amplified by PCR from pcDNA6/myc-His A (Life Technologies, Carlsbad, CA).

Transduction of MDCK Cells with Lentiviral Vectors

For production of lentiviruses, 293T cells were cotransfected with pCS-BS-shCtrl, or pCS-BS-shIRF7 together with the pCAG-HIVgp, pRSV-Rev (kind gifts from Dr. H. Miyoshi, RIKEN, Tsukuba) and pVSV-G (Clontech, Mountain View, CA) using FuGENE 6 (Roche Applied Science, Indianapolis, IN). Culture supernatants were collected 48 h after transfection and filtered. MDCK cells were transduced with these lentiviruses for 12 h in the presence of 8 μg/mL polybrene and cultured with fresh media. After 48 h of culture, the media were replaced with the selection media containing 10 μg/mL blastcidin S.

Quantitative Real-time One-step RT-RCR

Real-time RT-PCR reactions were carried out using TaqMan One-step RT-PCR Master Mix Reagents Kit (Applied Biosystems, Foster City, CA) according to the manufacture's instructions with a total volume of 25 μl. The primers and probes used for quantification of target mRNA were shown in Table 2. The total volume of 5 μl of sample RNA was added into 20 μl of reaction mix. Thermal cycling was performed in a Light Cycler 480 Real-time PCR system II (Roche Diagnostics, Germany) with conditions at 48°C for 30 min, 95°C for 10 min followed by 40 cycles at 95°C for 5 sec and 60°C for 1 min. The amount of target RNA was normalized with the amount of 18S rRNA from host cells or carrier RNA. The knockdown effect on the targeted gene by the specific siRNA was examined by real-time RT-PCR with power SYBR green PCR master mix (Applied Biosystems, Warrington, UK).

Reverse Transcription, Amplification, and Sequence Analysis of mRNA Expressed in MDCK Cells

Reverse transcription was performed using ReverTra-Ace (Toyobo, Osaka, Japan) with random hexamers and the thermal profiles consisted of one cycle at 37°C for 30 min, 42°C for 20 min, 99°C for 5 min and 4°C for 5 min. For detecting a canis lupus familiaris gene corresponding to human IRF7, the cDNA was amplified by KOD Dash polymerase (Toyobo, Japan) using primers shown in Table 2. Thermal cycling conditions were as follows: 30 cycles of 98°C for 10 sec, 55°C for 2 sec and 74°C for 5 min. PCR products were separated by electrophoresis at 100 V for 1 h in a 1.5% (wt/vol) agarose S (Nippon Gene, Tokyo, Japan) gel with TBE buffer and visualized by GelRed Nucleic Acid Gel Stain (Wako, Japan) under UV transillumination. The desired PCR products were extracted and purified using QIAquick gel extraction Kit (Qiagen, Hilden, Germany). The purified products were used for the reaction with BigDye Terminator cycle sequencing ready reaction kit version 3.0 (Applied Biosystems, Foster City, CA). Sequencing alignment was analyzed by using the software Sequencher 4.10.1 (Gene Codes, Ann Arbor, MI).

Network Analysis

The molecular interaction networks were analyzed by Ingenuity Pathway Analysis (IPA; Ingenuity Systems, Mountain View, CA).

Virus Infection and Hemagglutination (HA) Assay

The MDCK cells expressing shRNA for IRF7 or control were seeded on a 6-well plate at a density of 2×10^5 cells/well and cultured until confluent layers were obtained in Opti-pro SFM containing 10 μg/ml of blasticidin S. Cells were infected with indicated amount of PR8 (A/H1N1), NR1 (A/H1N1pdm09), VIC361 (A/H3N2), or FL4 (B/Yam) in Opti-Pro SFM at 34°C for 1 h. Then, cells were cultured with Opti-Pro SFM in the presence of 2 μg/ml of trypsin acetylated and incubated at 37°C for 48–96 h. The culture supernatants were collected for following HA assay. Red blood cells were purchased from Nippon Bio-Test Laboratories, Tokyo, Japan. Guinea pig red blood cells (GRBC) were washed three times with PBS and suspended in PBS at a final concentration of 1% as a working suspension. Turkey red blood cells (TRBC) or chicken red blood cells (CRBC) were washed with 0.85% NaCl and suspended in PBS at a final concentration of 0.5% as a working suspension. For NR1, the virus samples were diluted with PBS serially in U-bottom 96-well plates and then 50 μl of 0.5% TRBC suspension was added into each well and allowed to stand for 45 min at room temperature. For PR8 or VIC361, 50 μl of 1% GRBC suspension was added to serially diluted virus samples and allowed to stand for 60 min at 4°C. For FL4, 50 μl of 0.5% CRBC suspension was added to serially diluted virus samples and allowed to stand for 45 min at room temperature. The HA titer was determined as the highest dilution of the sample showing complete agglutination pattern on the bottom of the well.

Results

First siRNA Library Screening

The strategy to establish modified MDCK cells with higher efficiency of influenza virus propagation was summarized in the flowchart (Fig. 1). To identify key host factors in canine MDCK cells, we used A549 human lung adenocarcinoma cell line for the first screening because human genome database includes much more information than canis lupus familiaris genome database and related resources including pre-designed siRNA library are available in human.

We screened 78 human genes associated with type I IFN using siRNA library, for enhancement of the propagation of influenza A virus in A549 cells. The siRNAs for each target gene were individually transfected into A549 cells, and the cells were infected with influenza A/Puerto Rico/34/8 (PR8) at a MOI of 0.01. We used PR8 virus, because PR8 has suitable growth properties in many cell lines and is widely used as a backbone virus for the development of high growth reassortants for vaccine production [15]. In the first screening, when knockdown of a cellular gene by the corresponding siRNA showed more than 2-fold enhancement of virus propagation, the gene was considered positive (Fig. S1). A total of 23 out of 78 genes were chosen for further analysis to validate the positive effect of siRNA in influenza virus multiplication.

Knockdown of IRF7 Enhances the Production of PR8 Virus in A549 Cells

To understand which pathway is most important for improvement of viral propagation, we mapped the genes and their products identified in the type I IFN-related main pathways (Fig. 2A) and categorized these molecules into 3 groups (Fig. 2B). As the knockdown of NFKB1 enhanced the production of PR8 virus, we thought that NFKB1 might be one of the candidates. NFKB1 serves in downstream signaling pathways leading to the activation of type I IFN production and a common molecule in the three signaling pathways (Fig. 2A and B). Also, knockdown of TBK1, SMAD4 or IRF7 enhanced the production of PR8 virus (Figs. 2A and S1). Seventeen out of 23 genes were shown to be critically related to RIG-I/IPS-1-mediated type I IFN production (Fig. 2B). These results indicate that the genes mainly involved in